



Title	Pib2 is a cysteine sensor involved in TORC1 activation in <i>Saccharomyces cerevisiae</i>
Author(s)	Zeng, Qingzhong; Araki, Yasuhiro; Noda, Takeshi
Citation	Cell Reports. 2024, 43, p. 113599
Version Type	VoR
URL	https://hdl.handle.net/11094/93531
rights	This article is licensed under a Creative Commons Attribution 4.0 International License.
Note	

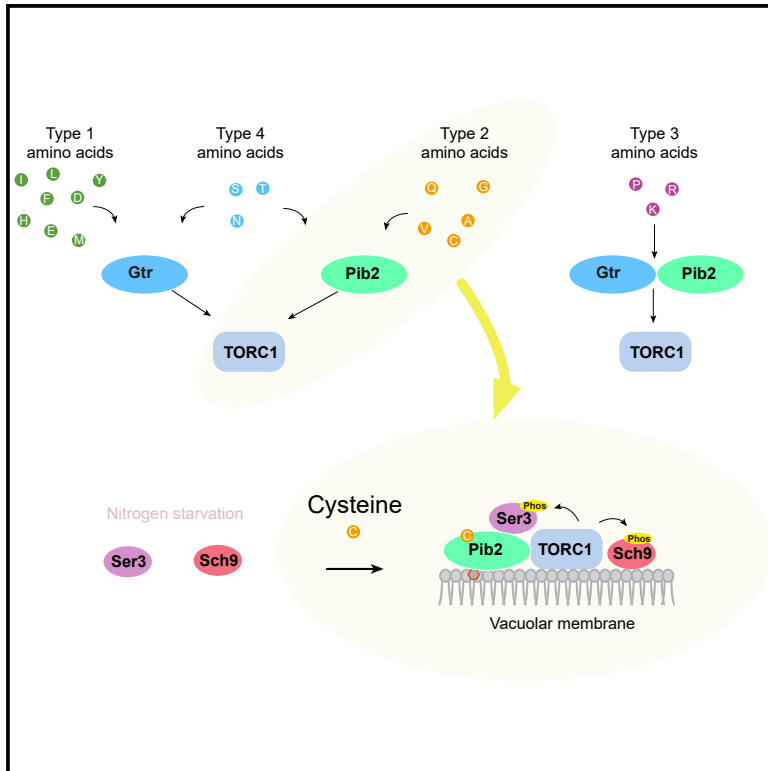
The University of Osaka Institutional Knowledge Archive : OUKA

<https://ir.library.osaka-u.ac.jp/>

The University of Osaka

Pib2 is a cysteine sensor involved in TORC1 activation in *Saccharomyces cerevisiae*

Graphical abstract



Authors

Qingzhong Zeng, Yasuhiro Araki,
Takeshi Noda

Correspondence

araki.yasuhiro.dent@osaka-u.ac.jp (Y.A.),
noda.takeshi.dent@osaka-u.ac.jp (T.N.)

In brief

Zeng et al. found that TORC1 activation by various amino acids differentially depends on Gtr or Pib2 pathways in *S. cerevisiae*. Cysteine directly binds to Pib2, and defective binding abrogates cysteine-dependent TORC1 activation.

Highlights

- TORC1 activation by various amino acids differentially depends on the Gtr or Pib2 pathways
- Cysteine directly binds to Pib2
- A binding defect abrogates cysteine-dependent TORC1 activation



Article

Pib2 is a cysteine sensor involved in TORC1 activation in *Saccharomyces cerevisiae*

Qingzhong Zeng,¹ Yasuhiro Araki,^{2,*} and Takeshi Noda^{1,2,3,4,*}
¹Graduate School of Frontier Biosciences, Osaka University, Osaka 565-0871, Japan

²Center for Frontier Oral Sciences, Graduate School of Dentistry, Osaka University, Osaka 565-0871, Japan

³Center for Infectious Disease Education and Research, Osaka University, Osaka 565-0871, Japan

⁴Lead contact

*Correspondence: araki.yasuhiro.dent@osaka-u.ac.jp (Y.A.), noda.takeshi.dent@osaka-u.ac.jp (T.N.)

<https://doi.org/10.1016/j.celrep.2023.113599>

SUMMARY

Target of rapamycin complex 1 (TORC1) is a master regulator that monitors the availability of various amino acids to promote cell growth in *Saccharomyces cerevisiae*. It is activated via two distinct upstream pathways: the Gtr pathway, which corresponds to mammalian Rag, and the Pib2 pathway. This study shows that Ser3 was phosphorylated exclusively in a Pib2-dependent manner. Using Ser3 as an indicator of TORC1 activity, together with the established TORC1 substrate Sch9, we investigated which pathways were employed by individual amino acids. Different amino acids exhibited different dependencies on the Gtr and Pib2 pathways. Cysteine was most dependent on the Pib2 pathway and increased the interaction between TORC1 and Pib2 *in vivo* and *in vitro*. Moreover, cysteine directly bound to Pib2 via W632 and F635, two critical residues in the T(aiI) motif that are necessary to activate TORC1. These results indicate that Pib2 functions as a sensor for cysteine in TORC1 regulation.

INTRODUCTION

Living organisms must be capable of sensing internal and external environmental changes promptly and efficiently and responding appropriately to these changes to maintain homeostasis. They achieve this through signaling cascades that rapidly and rigorously integrate numerous environmental inputs and transmit this information to metabolic regulators to control anabolic and catabolic processes. Target of rapamycin complex 1 (TORC1) or mechanistic TORC1 (mTORC1) is a master regulator of cell growth that is highly conserved across eukaryotes, and it responds to nutrient levels to coordinate metabolism and cell growth.^{1,2}

In the budding yeast *Saccharomyces cerevisiae*, TORC1 is comprised of a central protein kinase, either Tor1 or Tor2, in association with the accessory subunits Kog1, Tco89, and Lst8.¹ When amino acids are available, TORC1 promotes anabolic processes such as protein synthesis by phosphorylating Sch9, the homolog of S6 kinase (S6K) in mammals.^{3,4} At the same time, TORC1 suppresses catabolic processes such as autophagy by phosphorylating the autophagy-related protein Atg13.^{5,6} These effects are reversed during conditions of amino acid or nitrogen starvation; upon nitrogen starvation, Atg13 is dephosphorylated and enhances the formation of protein condensates termed the pre-autophagosomal structure/phagophore assembly site (PAS), which is comprised of most autophagy-related proteins, including Atg2.^{5,7–9}

TORC1 activity is regulated by the heterodimeric small GTPases Gtr1-Gtr2 (the Gtr complex) in *S. cerevisiae* or its mammalian orthologs RagA/B-RagC/D (the Rag complex).^{10,11} In mammals, the Rag complex is anchored to the lysosomal membranes via the Ragulator complex.¹² When RagA/B takes the GTP-bound form to recruit mTORC1 to lysosomes, the small GTPase Rheb encounters mTORC1, which is thereby activated.¹³ Several amino acids activate mTORC1 by blocking GATOR1, which is a GTPase-activating protein (GAP) for RagA/B.^{14,15} Upon amino acid deprivation, the activation of GATOR1 promotes RagA/B to take the GDP-bound form, resulting in inactivation of mTORC1.¹⁴ Under amino-acid-rich conditions, GATOR1 is suppressed by its negative regulator, GATOR2.¹⁴ In *S. cerevisiae*, the Gtr complex is anchored to vacuolar membranes via the EGO complex, which consists of Ego1, Ego2, and Ego3 and possesses a similar architecture to Ragulator.^{10,16} The functional counterparts of GATOR1 and GATOR2 in budding yeast are SEACAT and SEACIT, respectively.^{17–20} SEACIT acts as a GAP for Gtr1 and inactivates TORC1, while SEACAT inhibits SEACIT. Unlike the dissociation from lysosomes in mammals, inactivated TORC1 forms puncta that associate with vacuoles, and activated TORC1 disperses on the vacuolar membrane.^{20,21} It is still uncertain whether a functional counterpart of Rheb exists in budding yeast.

Recently, there has emerged a class of proteins that function as amino acid sensors in mammals. Sestrin2 was the first leucine sensor to be identified. When leucine is abundant, Sestrin2 binds



to leucine and becomes unable to bind to GATOR2, which enables GATOR2 to function as a GATOR1 inhibitor, leading to mTORC1 activation.²² Several other amino acid sensors have been reported: CASTOR, an arginine sensor; SAMTOR, a methionine (SAM) sensor; and SAR1B, another leucine sensor.^{23–25} Although these findings have advanced our understanding of how mammalian cells respond to amino acid availability, these amino acid sensors are not conserved in the budding yeast.

Pib2 was recently characterized as a TORC1 regulator that functions outside of the Gtr pathway in *S. cerevisiae*.^{26–29} It also associates with the vacuolar membrane via its FYVE domain, which interacts with phosphatidylinositol 3-phosphate (PtdIns3P).^{26–29} Cells deficient in Gtr1 or Pib2 alone are still able to grow, but double knockout leads to synthetic lethality.^{26,29} Conditional mutations in Gtr1 and Pib2 resulted in the loss of TORC1 activity.²⁸ The above studies indicate that TORC1 activation occurs through two parallel upstream pathways, the Gtr pathway and the Pib2 pathway. Interestingly, Pib2 serves as a main component of the glutamine sensor, and glutamine facilitates Pib2-TORC1 interaction to activate TORC1.^{28,30} Despite these reports, the molecular mechanisms by which individual amino acids activate TORC1 remain largely unclear, especially in budding yeast.

There are at least two separate phases whereby amino acids activate TORC1 after nitrogen starvation: phase 1 involves acute, transient activation at around 5 min, and phase 2 is characterized by slow, continuous activation later than 15 min.^{12,31} In phase 2, prototrophic yeast is able to convert any amino acid to any other amino acids through metabolic reactions. Auxotrophy in the parental strain can result in potential bias when analyzing physiological quantitative parameters in metabolic networks. By contrast, in phase 1, TORC1 may react to individual amino acid species before they are metabolized. Therefore, we studied brief amino acid stimulation to investigate how TORC1 monitors individual amino acids.

Using the well-established TORC1 substrate Sch9 and the uncharacterized TORC1 substrate Ser3, the latter of which is specifically phosphorylated by the Pib2 pathway, we analyzed the relationships between 20 amino acids and the Gtr and Pib2 pathways. We discovered that cysteine activates TORC1 in a manner dependent on the Pib2 pathway and enhances Pib2-TORC1 interaction by directly binding to Pib2. Thus, Pib2 serves as a cysteine sensor in the TORC1 pathway.

RESULTS

Identification of Ser3 as a Pib2-pathway-specific TORC1 substrate

We analyzed our previous mass spectrometry (MS) data of the proteins co-immunoprecipitated by TAP-Pib2²⁸ and noticed that both Ser3 and its paralog, Ser33, were present at high levels (Figure S1A). This relationship was also observed in a recent Pib2-interactome study.³² Both Ser3 and Ser33 are 3-phosphoglycerate dehydrogenases that catalyze the first step in serine and glycine biosynthesis.³³ It was previously shown that GFP-Tor1 protein formed puncta in the vicinity of the vacuolar membrane in *gtr1Δ* cells.^{20,21} In this study, Ser3-GFP and Ser33-GFP also formed puncta in *gtr1Δ* cells, and the puncta disappeared after being distributed throughout the cytoplasm by exogenously expressed

GTR1 (Figures 1A and S1B). When compared with the TORC1 subunit Tco89-mCherry, these Ser3-GFP and Ser33-GFP puncta in *gtr1Δ* cells completely overlapped (Figure 1B). These findings suggest an association of TORC1 with Ser3 and Ser33 via Pib2.

We then sought to determine if TORC1 directly phosphorylates Ser3. First, recombinant 6His-Ser3 was expressed and purified from *Escherichia coli*. Next, TAP-tagged GFP-Tor1^{I1954S}, which is a hyperactive Tor1 mutant,²⁹ was purified from yeast. When these proteins were incubated *in vitro* in the presence of ATP and then subjected to SDS-PAGE containing Phos-tag reagent to expand the phosphorylation-dependent band shift, the Ser3 band was clearly upshifted (Figure 1C). Thus, Tor1 can directly phosphorylate Ser3.

In wild-type cells, Sch9 was phosphorylated under nutrient-rich growing conditions, as detected by phosphor-specific Sch9 (T737) antibody (Figure 1D).^{3,34} This phosphorylation was suppressed by treatment with rapamycin, a TORC1 inhibitor, and enhanced by cycloheximide, a TORC1 activator (Figure 1D).^{10,35} Although simultaneous abrogation of the Gtr and Pib2 pathways led to complete abolition of Sch9 phosphorylation,²⁸ this phosphorylation was only slightly suppressed by *gtr1Δ* or *pib2Δ* cells individually (Figure 1D), indicating that TORC1 can phosphorylate Sch9 either via the Gtr pathway or the Pib2 pathway. The upshifted phosphorylated band of Ser3-3HA was suppressed by rapamycin treatment and enhanced by cycloheximide treatment (Figure 1D), indicating that Ser3 is a bona fide TORC1 substrate. Ser3 phosphorylation was observed in untreated *gtr1Δ* cells and was further enhanced by cycloheximide treatment (Figure 1D). In sharp contrast, Ser3 phosphorylation was totally suppressed during growth conditions in *pib2Δ* cells, even after cycloheximide treatment (Figure 1D). These results indicate that Ser3 is a specific substrate of the Pib2-dependent pathway.

TORC1 activation by methionine and cysteine depends mainly on the Gtr pathway and the Pib2 pathway, respectively

We explored the relationships of individual amino acids with the Gtr and Pib2 pathways. To avoid bias related to auxotrophy, a prototrophic strain was prepared by introducing a plasmid expressing all auxotrophic markers.³⁶ We monitored the status of TORC1 activity by detecting the phosphorylation of two TORC1 substrates, Sch9 and Ser3. Following 30 min nitrogen starvation, TORC1 activity was monitored from 3 until 12 min after stimulation with amino acids. Twenty amino acids were individually added to wild-type, *pib2Δ*, or *gtr1Δ* cells at a concentration of 5 mM, which is sufficient to activate TORC1 in *S. pome*,³⁷ and the cells were then harvested at various time points (Figure 2A). While Sch9 phosphorylation occurred after the addition of methionine to wild-type cells and *pib2Δ* cells (Figure 2B), it barely occurred in *gtr1Δ* cells (Figure 2B). Methionine also induced Ser3 phosphorylation in wild-type cells but not in *gtr1Δ* cells (Figure 2B). In contrast, the addition of cysteine induced Sch9 phosphorylation in wild-type and *gtr1Δ* cells but significantly decreased this phosphorylation in *pib2Δ* cells (Figure 2C). Ser3 phosphorylation was observed in *gtr1Δ* cells with the addition of cysteine (Figure 2C). These phosphorylation events were sensitive to rapamycin treatment, indicating that they are TORC1 dependent (Figures S1C and S1D). Collectively, these results

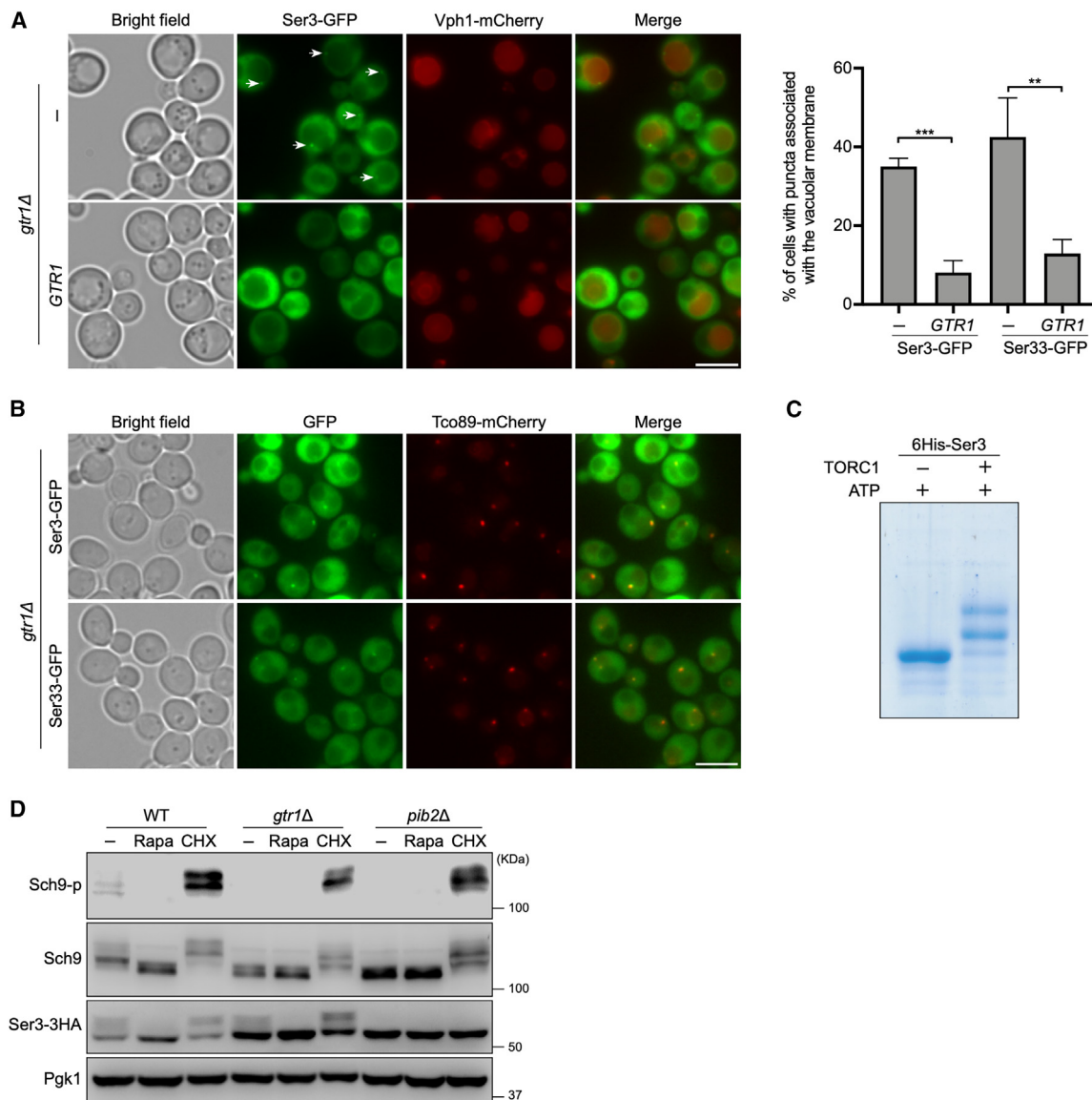


Figure 1. Ser3 is specifically phosphorylated by TORC1 in the Pib2 pathway

(A) *gtr1Δ* cells (YAY2674) expressing pRS316 or pRS316-*GTR1* were grown in SCD medium and analyzed by fluorescence microscopy. Arrows indicate Ser3-GFP puncta. Scale bar: 5 μ m. The percentages of cells with vacuolar membrane-associated puncta were calculated (right). Data represent the means \pm SD from three independent experiments ($n > 100$). Unpaired t test. ** $p < 0.01$, *** $p < 0.001$.

(B) *gtr1Δ* cells expressing Tco89-mCherry and either Ser3-GFP (YAY3071) or Ser33-GFP (YAY3072) were grown at 30°C in SCD medium and observed by fluorescence microscopy. Scale bar: 5 μ m.

(C) GFP-tagged *TOR1^{I1954S}*-expressing cells (YAY2838) were subjected to immunoprecipitation with GFP-Trap beads and a TORC1 kinase assay using 6His-Ser3 purified from *E. coli* as a substrate. The samples were separated on SDS-PAGE with 20 μ M Phos-tag and stained with Coomassie brilliant blue (CBB).

(D) Wild-type (YAY2864), *gtr1Δ* (YAY2867), and *pib2Δ* (YAY2868) cells grown in YPD medium were treated with 0.2 μ g/mL rapamycin (Rapa) or 25 μ g/mL cycloheximide (CHX) for 30 min. Cell lysates were analyzed by western blotting using anti-Sch9-p (T737), anti-Sch9, anti-HA, and anti-Pgk1 antibodies.

suggested that methionine-induced TORC1 activation is more dependent on the Gtr pathway, while cysteine activation of TORC1 is more dependent on the Pib2 pathway.

TORC1 localization is correlated with its activity; specifically, it is activated when distributed throughout the vacuolar membrane.^{20,21,38} Under nitrogen starvation, GFP-Tor1 forms puncta proximal to the vacuolar membrane, and TORC1 activity is sup-

pressed. When cysteine or methionine was added to starved cells in this study, the GFP-Tor1 puncta became dispersed throughout the vacuolar membrane in wild-type cells (Figure S1E). In *pib2Δ* cells, the addition of methionine decreased the number of GFP-Tor1 puncta, but the addition of cysteine did not (Figure S1E). In *gtr1Δ* cells, on the other hand, the addition of cysteine significantly reduced the number of GFP-Tor1 puncta, whereas the addition of

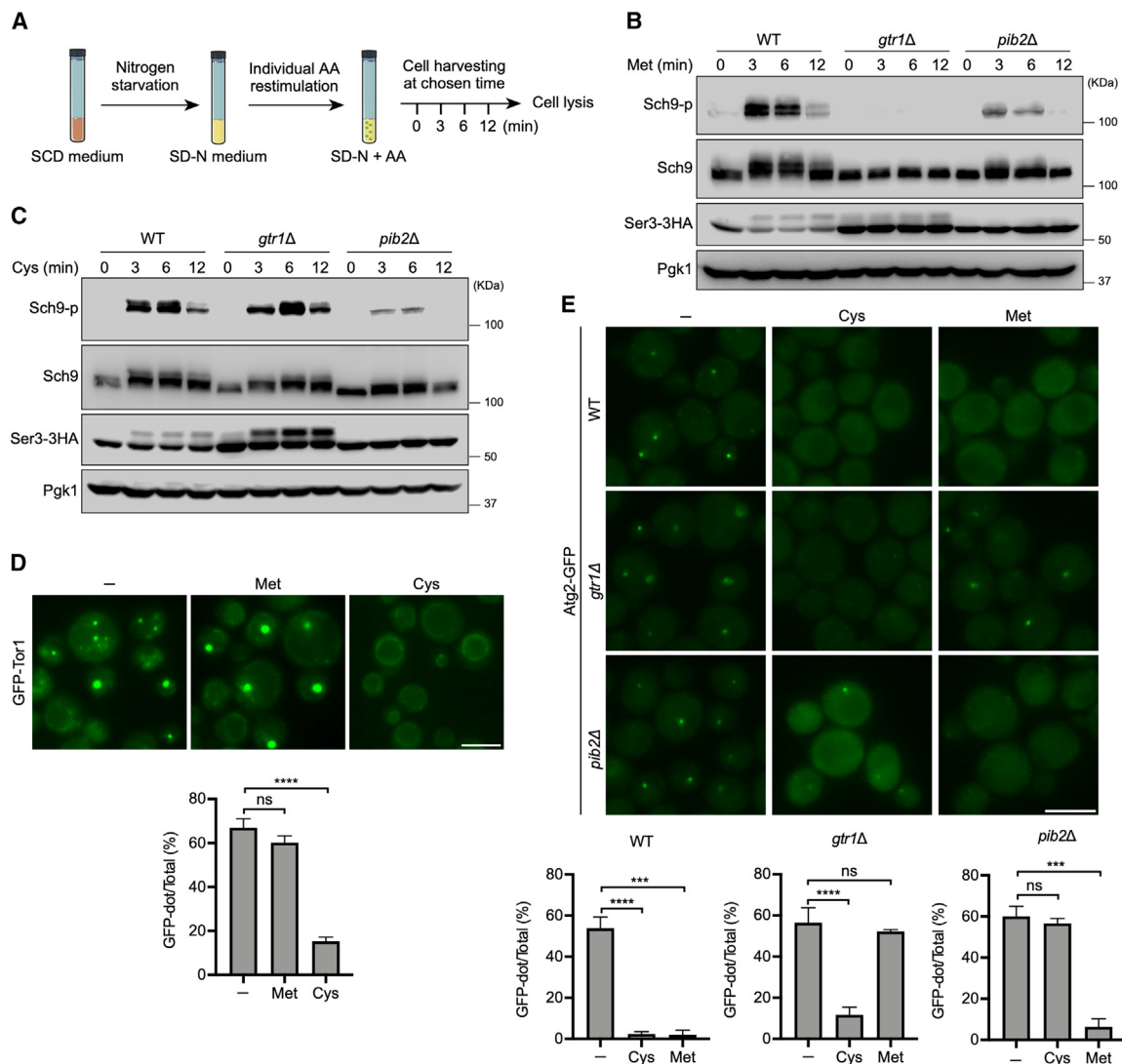


Figure 2. TORC1 activation by methionine and cysteine is highly dependent on the Gtr and Pib2 pathways, respectively

(A) A restimulation assay of individual amino acids (aa) in wild-type (WT) (YAY2864), *gtr1Δ* (YAY2867), and *pib2Δ* (YAY2868) cells. Cells were grown in SCD medium until the exponential growth phase, shifted to SD-N medium for nitrogen starvation for 30 min, supplemented with a 5 mM concentration of each aa, and harvested at the indicated time points.

(B and C) WT (YAY2864), *gtr1Δ* (YAY2867), and *pib2Δ* (YAY2868) cells were grown as in (A); 5 mM methionine (B) or cysteine (C) was added, and the cells were harvested at the indicated time points. Lysates were analyzed by western blotting.

(D) *gtr1Δ* cells expressing GFP-Tor1 (ZQZ102) were nitrogen starved for 30 min and replenished with methionine or cysteine for 6 min. Scale bar: 5 μ m. The percentages of cells with vacuolar membrane-associated GFP-Tor1 puncta were calculated (bottom). The graph shows the means \pm SD from three independent experiments ($n > 60$). Unpaired t test. ns, no significance, **** $p < 0.0001$.

(E) *gtr1Δ* cells expressing Atg2-GFP (WT: ZQZ148, *gtr1Δ*: ZQZ150, *pib2Δ*: ZQZ152) were nitrogen starved for 30 min (–) and then stimulated with cysteine or methionine for 6 min. Scale bar: 5 μ m. The percentages of cells exhibiting Atg2-GFP puncta were calculated (bottom). The graph shows the means \pm SD from three independent experiments ($n > 55$). Unpaired t test. ns, no significance, *** $p < 0.001$, **** $p < 0.0001$.

methionine did not (Figure 2D). Additionally, Pib2 localization has been reported to be correlated with TORC1 activity.²⁸ GFP-Pib2 puncta are associated with vacuoles in *gtr1Δ* cells under nitrogen starvation, and their number decreased with the addition of cysteine but not methionine (Figure S1F). Autophagy occurs downstream of TORC1, and Atg2 is recruited to puncta called the PAS when TORC1 is inactivated under starvation.^{6,39} When

cysteine was added after starvation, the number of Atg2-GFP puncta was decreased in wild-type cells and *gtr1Δ* cells but not in *pib2Δ* cells (Figure 2E). In contrast, the addition of methionine decreased the number of Atg2-GFP puncta in *pib2Δ* cells and wild-type cells but not in *gtr1Δ* cells (Figure 2E).

Collectively, these results reinforce the conclusion that methionine-induced TORC1 activation is mainly dependent on the Gtr

pathway, while cysteine activation of TORC1 depends more on the Pib2 pathway.

Amino acids differ in their dependencies on the Gtr and Pib2 pathways in TORC1 activation

We next examined amino acids other than methionine and cysteine. In the case of lysine, the phosphorylation level of Sch9 was significantly decreased in both *gtr1Δ* cells and *pib2Δ* cells (Figure 3A), suggesting that lysine activates TORC1 through both the Gtr and Pib2 pathways.

Serine was able to induce Sch9 phosphorylation in wild-type cells (Figure 3B). Even in *gtr1Δ* or *pib2Δ* cells, Sch9 was phosphorylated with the addition of serine, and Ser3 was phosphorylated in *gtr1Δ* cells (Figure 3B). Based on this result, we considered it possible that serine activates TORC1 through a third pathway. However, when both the Gtr and Pib2 pathways were simultaneously abrogated in *gtr1Δ ego1Δ* with temperature-sensitive *pib2* cells,²⁸ serine did not induce phosphorylation of Sch9 and Ser3 at the restrictive temperature of 37°C (Figure 3C). These results indicate that serine can activate TORC1 by either the Gtr or Pib2 pathway.

Based on these criteria, 20 amino acids were divided into four types. Type 1 includes amino acids more dependent on the Gtr pathway: Met, Leu, Ile, Glu, Asp, His, Phe, Tyr, and Trp. As shown in the case of Met (Figure 2B), Sch9 phosphorylation was induced by these amino acids in *pib2Δ* cells but only minimally in *gtr1Δ* cells (Figures 3D and S2A). These amino acids did not induce significant Ser3 phosphorylation in *gtr1Δ* cells (Figures 2B, S2B and S2C). Type 2 includes amino acids more dependent on the Pib2 pathway: Cys, Gly, Gln, Val, and Ala. As shown in the case of Cys (Figure 2C), Sch9 phosphorylation occurred in *gtr1Δ* cells but was significantly reduced in *pib2Δ* cells (Figures 3D, S2A). These amino acids also efficiently induced Ser3 phosphorylation in *gtr1Δ* cells (Figures 2C, S2B, and S2C). Type 3 includes amino acids dependent on both the Gtr and Pib2 pathways: Lys, Pro, and Arg. As shown in the case of Lys (Figure 3A), Sch9 phosphorylation was significantly decreased in *gtr1Δ* cells and *pib2Δ* cells compared to wild-type cells (Figures 3D and S2A). These amino acids did not significantly induce Ser3 phosphorylation in *gtr1Δ* cells (Figures 3B, S2B, and S2C). Type 4 includes amino acids dependent on either the Gtr or Pib2 pathway: Ser, Asn, and Thr. As shown in the case of Ser (Figure 3B), Sch9 was efficiently phosphorylated in both *gtr1Δ* cells and *pib2Δ* cells (Figures 3B, 3D, and S2A). These amino acids also efficiently induced Ser3 phosphorylation in *gtr1Δ* cells (Figures 3B, S2B, and S2C). We confirmed that Asn and Thr did not induce Sch9 or Ser3 phosphorylation in *gtr1Δ ego1Δ* with temperature-sensitive *pib2* cells at 37°C (Figures S2D and S2E).

Collectively, these data suggest that there are differences between amino acids regarding their dependencies on the two pathways of TORC1 activation.

Cysteine activates TORC1 via the Pib2 pathway

Of the aforementioned results, we focused on the fact that cysteine exerted the most prominent effect on TORC1 activation in *gtr1Δ* cells (Figures 3D and S2C). This was based on a comparison of the responses of wild-type and *gtr1Δ* cells to each amino acid. In order to compare each amino acid more directly, we

observed the responses of *gtr1Δ* cells to all amino acids in the same blot. After nitrogen starvation, each amino acid was added individually for 6 min. Type 2 (Pib2) and type 4 (Gtr or Pib2) amino acids induced Sch9 and Ser3 phosphorylation (Figures 3D–3F, S3A, and S3B). Some amino acids alone caused greater phosphorylation than all amino acids together because when amino acids were added individually, their concentrations were higher (0.5–1.0 mM) than when all amino acids were included in the medium (Table S1). Although we did not evaluate if multiple amino acids exerted a cooperative effect, the total concentration of all type 2 amino acids was 3.6 mM, which is lower than that of cysteine alone (5 mM). In agreement with the previous results, cysteine resulted in the most significant phosphorylation of both Sch9 and Ser3 in *gtr1Δ* cells (Figures 3E, 3F, S3A, and S3B). Likewise, the formation of GFP-Tor1 puncta under nitrogen starvation was more effectively decreased by cysteine than by any of the other type 2 amino acids, including glutamine, as we previously reported (Figure S3C).²⁸ The formation of GFP-Tor1 puncta was also decreased by the readdition of cysteine within 6 min after nitrogen starvation, and it gradually resumed over time (Figure S3D). A time course analysis of cysteine-induced TORC1 activation showed that Sch9 and Ser3 phosphorylation peaked at 6 min after cysteine addition and then started to decrease (Figure S3E). A concentration-dependency analysis showed that the addition of 50–100 μM cysteine induced minimal TORC1 activity, and this activity was mostly saturated at 5 mM (Figure S3F).

It is possible that *pib2Δ* cells do not sufficiently take up cysteine from the medium, leading to impaired TORC1 activation. In fact, it has been reported that Gtr affects the functional localization of Gap1, a general amino acid permease, at the plasma membrane.^{40,41} To assess this possibility, we measured [³⁵S]-cysteine uptake into cells. As controls, *gap1Δ* cells and *yct1Δ* cells (Yct1 is a high-affinity cysteine-specific transporter)^{42,43} obviously reduced cysteine uptake (Figure 3G). However, *pib2Δ* cells did not exhibit defective uptake (Figure 3G). Further, we confirmed that Gap1-GFP and Yct1-GFP localized normally at the plasma membrane in both *pib2Δ* cells and wild-type cells (Figures S3G and S3I). These results ruled out the possibility that the defective cysteine-induced TORC1 activation in *pib2Δ* cells is due to inefficient cysteine uptake.

Glutathione is a downstream metabolite of cysteine. To determine whether TORC1 is activated indirectly after conversion into glutathione, we examined a deletion mutant of gamma glutamyl-cysteine synthetase, encoded by *GSH1*, which catalyzes the first step in glutathione biosynthesis.⁴⁴ However, cysteine-dependent TORC1 activation was not affected in *gsh1Δ* cells (Figure S3H), and glutathione addition did not promote TORC1 activation (Figure S3H). These results indicated that the activation of TORC1 by cysteine is not mediated through its conversion into glutathione.

Altogether, these data demonstrate that cysteine-induced TORC1 activation is primarily mediated by the Pib2 pathway.

Cysteine promotes Pib2-TORC1 interaction *in vivo*

Since previous studies showed that Pib2 associates with TORC1,^{27,28} we investigated whether cysteine affects this interaction. The amount of Tor1 that co-precipitated with GFP-Pib2 was greater after the addition of cysteine to the medium than in cells

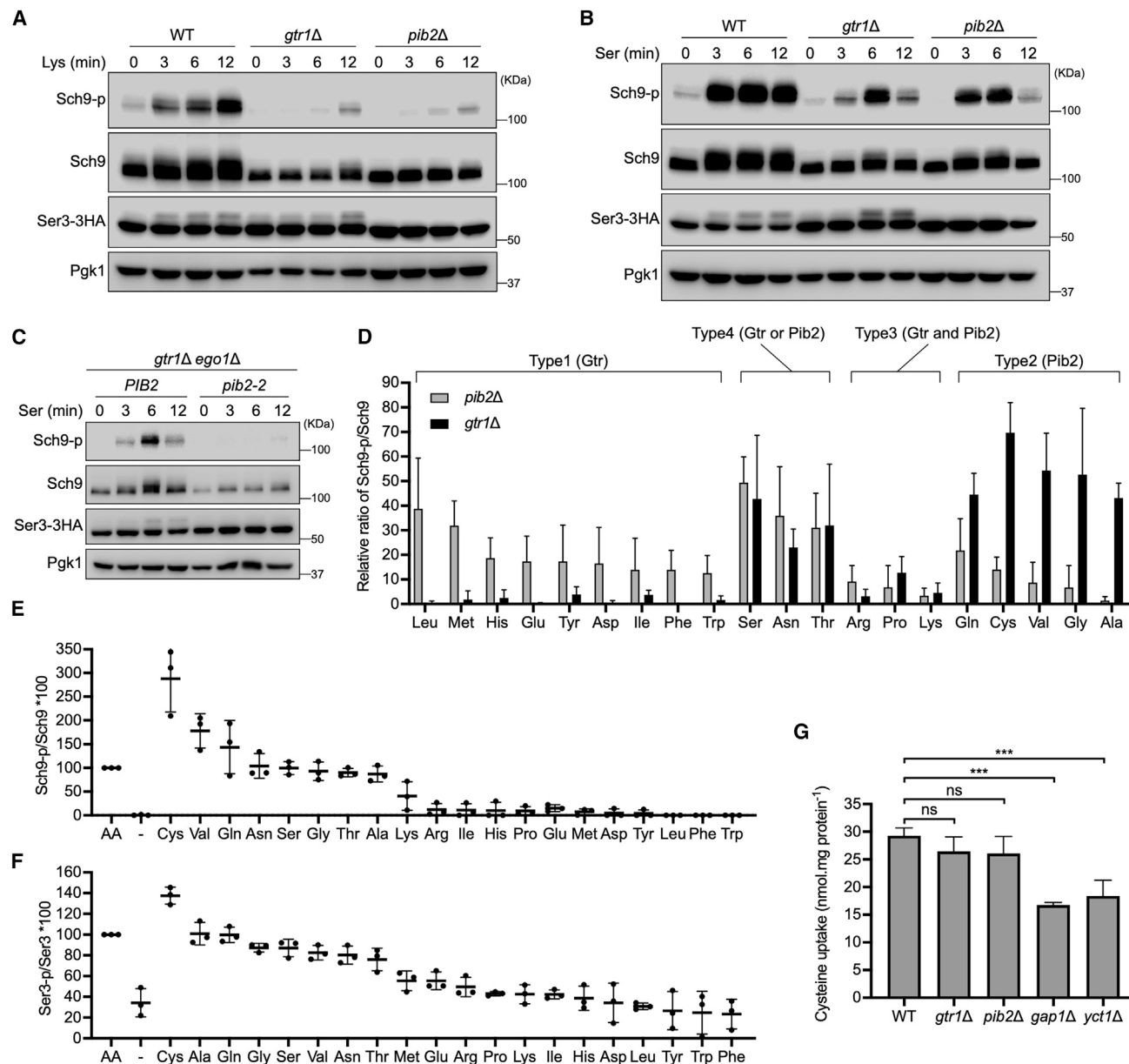


Figure 3. Classification of aa according to dependencies on the Gtr and Pib2 pathways

(A and B) WT (YAY2864), *gtr1Δ* (YAY2867), and *pib2Δ* (YAY2868) cells were grown as in Figure 2A; 5 mM lysine (A) or serine (B) was added, and the cells were harvested at the indicated time points. Lysates were analyzed by western blotting.

(C) *gtr1Δ ego1Δ* cells (PIB2: ZQZ108 or *pib2-2*: ZQZ109) expressing Ser3-3HA were nitrogen starved for 30 min and cultured with serine at 37°C for the indicated periods.

(D) Cells (YAY2864, YAY2867, and YAY2868) were cultured as in Figures 2A, and 5 mM each aa was added. See Figure S2A for immunoblotting data. The average band intensities of Sch9 phosphorylation at 3 and 6 min relative to the band intensities of Sch9 are presented. The means \pm SD of three independent biological replicates are shown.

(E and F) *gtr1Δ* cells (YAY2867) were nitrogen starved for 30 min and supplemented with a 5 mM concentration of each aa or complete aa for 6 min. See Figures S3A and S3B for immunoblotting data. The ratio of the band intensity of Sch9-p/Sch9 (E) and Ser3-p/Ser3 (F) of each aa relative to that of complete aa is presented. The means \pm SD of three independent biological replicates are shown.

(G) Cells (WT: YAY2864; *gtr1Δ*: YAY2867; *pib2Δ*: YAY2868; *gap1Δ*: ZQZ232; *yct1Δ*: ZQZ233) were starved of nitrogen for 30 min and then added to 0.5 μ M L-[³⁵S] cysteine and incubated for 5 min. The cells were collected, and the amount of intracellular L-[³⁵S]cysteine was determined. The graph represents means \pm SD from three independent experiments. Unpaired t test. ns, no significance, ***p < 0.001.

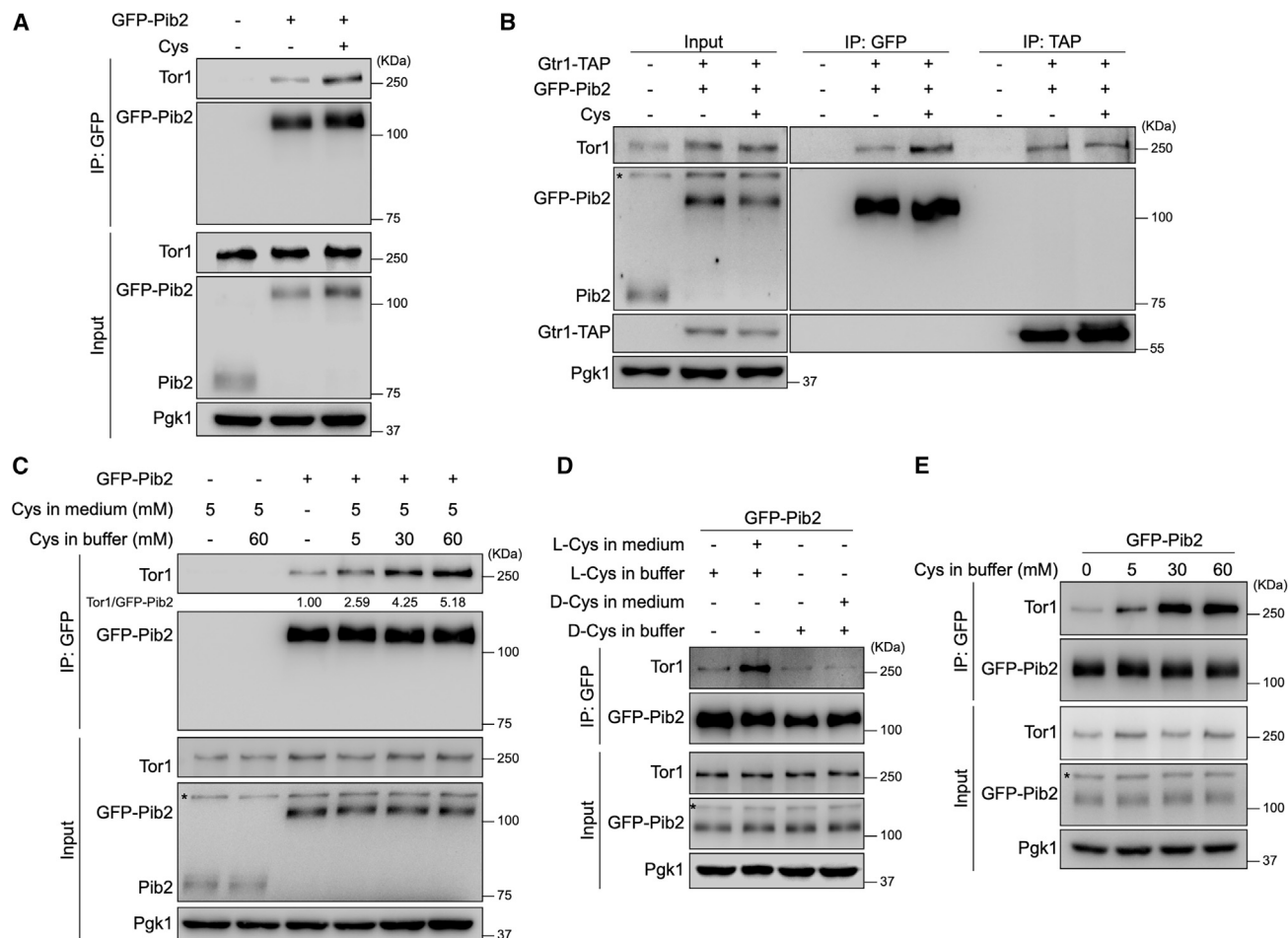


Figure 4. Cysteine promotes Pib2-TORC1 interaction *in vivo*

(A) Cells (ZQZ114) were nitrogen starved for 30 min and then incubated with or without 5 mM cysteine for 15 min. Cellular extracts were immunoprecipitated by GFP-Trap. Whole-cell extracts and precipitated proteins were analyzed by western blotting using anti-Tor1, anti-Pib2, and anti-Pgk1 antibodies.

(B) Cells (ZQZ116) were cultured as in (A). Extracts were prepared and immunoprecipitated by GFP-Trap or immunoglobulin G (IgG)-Dynabeads. Whole-cell extracts and precipitated proteins were analyzed by immunoblotting using anti-Tor1, anti-Pib2, anti-TAP, and anti-Pgk1 antibodies. The asterisk indicates non-specific bands.

(C) Cells (ZQZ114) were treated as in (A), and the indicated concentrations of cysteine were added to the immunoprecipitation buffer. The asterisk indicates non-specific bands.

(D) Cells (ZQZ114) were subjected to 30 mM L-cysteine or D-cysteine in the immunoprecipitation buffer, as in (C). The asterisk indicates non-specific bands.

(E) Cells (ZQZ114) were nitrogen starved for 30 min. Extracts were prepared and immunoprecipitated with GFP-Trap, and then the indicated concentrations of cysteine were added to the immunoprecipitation buffer.

under starvation conditions (Figure 4A). By contrast, the interaction between Gtr1 and TORC1 was not enhanced by cysteine addition (Figure 4B). When cysteine was added to immunoprecipitation buffers, Pib2-Tor1 interaction was further promoted in a dose-dependent manner (Figure 4C). The inclusion of cysteine in lysis buffer also enhanced this interaction (Figure S4A).

Although D-cysteine shares chemical properties with its enantiomer L-cysteine, only L-cysteine is utilized in cellular processes, including TORC1 activation via the Pib2 pathway (Figure S4B). D-cysteine did not promote Pib2-TORC1 interaction, unlike L-cysteine (Figure 4D). Leucine, a type 1 (Gtr) amino acid, did not enhance this interaction (Figure S4C). The addition of cysteine to all immunoprecipitation assay buffers enhanced Pib2-TORC1

interaction in a dose-dependent manner (Figures 4E and S5A), whereas D-cysteine and L-methionine did not (Figures S5B and S5C). Although glutamine has already been reported to enhance this interaction,^{28,30} we did not observe enhancement by glycine, another type 2 amino acid, in immunoprecipitation (IP) buffer. These results suggest that L-cysteine enhances Pib2-TORC1 interaction quite specifically.

Cysteine directly promotes Pib2-TORC1 interaction *in vitro*

To identify additional factors involved in this cysteine-dependent process, we analyzed proteins that co-immunoprecipitated with GFP-Pib2, with or without cysteine addition, followed by liquid

chromatography-tandem MS (LC-MS/MS). Consistent with the above results, GFP-Pib2 co-immunoprecipitated all the subunits of TORC1, namely Tor1, Tor2, Kog1, Tco89, and Lst8, and their amounts were increased with the addition of cysteine (Figure S5D). Following LC-MS/MS, we selected the other 55 proteins whose amounts changed upon cysteine addition and analyzed the effects of their deletion on the activation of TORC1 by cysteine. However, no factors affecting the cysteine-dependent response were identified.

Based on this outcome, we hypothesized that cysteine may activate TORC1 via Pib2 without additional factors. We then aimed to perform a pull-down assay with recombinant Pib2 proteins *in vitro* but did not obtain a sufficient amount of full-length recombinant Pib2 protein. Therefore, we sought to identify the region of Pib2 that is required for the cysteine-dependent activation of TORC1 in yeast. Pib2 is a 635-amino-acid protein that contains two highly conserved motifs, namely the FYVE domain and the tail (T) motif, as well as five motifs, designated A to E, that are weakly evolutionally conserved (Figure 5A).²⁹ In cells expressing a series of truncated Pib2 fused to GFP in *pib2Δ* cells, the addition of cysteine failed to activate TORC1 in GFP-Pib2(440–635) lacking motifs A to E (Figures 5A and 5B). Similarly, cysteine addition did not activate TORC1 in GFP-Pib2(1–620)-expressing cells, which lack the T motif (Figures 5A and 5B). However, GFP-Pib2(304–635), which contains only the E motif to the T motif, responded to cysteine activation of TORC1 (Figures 5A and 5B). These data indicated that the regions from the E motif to the T motif of Pib2 are necessary and sufficient for TORC1 activation by cysteine.

Hence, we purified GST-Pib2(304–635) from *E. coli*, which resulted in improved solubility and stability of the recombinant Pib2 protein (Figure 5C). We also purified TAP-Tor1 from a yeast strain (Figure 5C) and incubated it with GST-Pib2(304–635) *in vitro* with or without cysteine. TAP-Tor1 did not co-precipitate GST-Pib2(304–635) without cysteine, but cysteine supplementation facilitated the association of GST-Pib2(304–635) with TAP-Tor1 (Figures 5D and 5E). The addition of D-cysteine or L-methionine did not promote this interaction (Figure 5F). The Pib2(304–635)-TORC1 interaction was enhanced in a cysteine-dose-dependent manner *in vitro* (Figure 5G). These results demonstrate that this cysteine-induced interaction *in vitro* requires the presence of only Pib2 and TORC1.

Cysteine binds directly to Pib2

Given the above results, we hypothesized that cysteine might bind directly to Pib2. To examine this possibility, we performed an equilibrium binding assay *in vitro*.²² Radiolabeled cysteine was added to purified GST-Pib2(304–635), and it bound to GST-Pib2(304–635) but not to control GST protein (Figure 6A). Excess non-radiolabeled cysteine competed for this binding (Figure 6A). Serial dilution of non-labeled cysteine revealed that the dissociation constant (K_D) of the cysteine-Pib2 interaction was 136.5 μ M (Figure 6B). These results established that cysteine binds directly to Pib2.

The cysteine-binding residues of Pib2 are essential for cysteine activation of TORC1

Subsequently, we sought to determine which region of Pib2 is required for the cysteine-enhanced Pib2-TORC1 interaction.

Cysteine promoted the interaction of TORC1 with GFP-Pib2 (304–635), but not mutants lacking either the E motif (440–635) or the T motif (304–620) (Figures 6C and 6D), indicating that both the E and T motifs of Pib2 are required for the cysteine-dependent interaction with TORC1 *in vitro*. To further confirm which region of Pib2 binds to cysteine, we purified a series of GST-Pib2 truncation proteins and incubated them with radiolabeled cysteine in an equilibrium binding assay. Radiolabeled cysteine bound to GST-Pib2(440–635), which contains only the FYVE domain and the T motif, and this binding was competitively inhibited by excess non-radiolabeled cysteine (Figure 6E). However, Pib2(304–620) lacking the T motif was unable to bind radiolabeled cysteine (Figure 6E). Taken together, these results indicate that the T motif of Pib2 is critical for the binding of cysteine to Pib2.

The primary sequence of the T motif is well conserved in fungi (Figure 7A). To determine the critical residues in this motif, every three consecutive amino acids were replaced with three alanines (alanine was mutated to aspartic acid). As a result, the activation of TORC1 by cysteine was suppressed in cells expressing Pib2 mutants, whose residues 630–632 or 633–635 were mutated to three alanines (Figure 7B). Further alanine scanning within Pib2 residues 630–635 identified two residues, W632 and F635, that are critical for the activation of TORC1 by cysteine (Figure 7C). Although other residues also decreased phosphor-Sch9 to some degree, this may reflect a reduction in the amount of Sch9 by an unknown mechanism. These residues were perfectly evolutionally conserved among the referred fungi species (Figure 7A).

Radioactive cysteine bound specifically to GST-Pib2(304–635), but this binding was significantly abolished by either W632A or F635A mutation (Figure 7D), indicating that these residues are crucial for cysteine binding. The alanine substitutions in W632A and F635A significantly abrogated TORC1 activation by cysteine in yeast (Figure 7E). However, these mutations did not affect the activation of TORC1 by methionine (type 1) or several other type 2 amino acids, namely glutamine, valine, glycine, and alanine (Figures 7E and S6A–S6D). After nitrogen starvation, cysteine addition led to a reduction in GFP-Pib2 puncta formation in wild-type cells. However, this effect was not observed in *pib2Δ* mutants that expressed GFP-Pib2 W632A or GFP-Pib2 F635A and that lacked the entire T motif (Figures 7F and 7G). In summary, these results demonstrate that the W632 and F635 residues of Pib2 are critical for its binding to cysteine and for cysteine-dependent TORC1 activation.

DISCUSSION

In this study, we proposed that Pib2 serves as a cysteine sensor that contributes to TORC1 regulation in the yeast *S. cerevisiae*.

Cysteine was previously shown to activate TORC1 *in vitro*.^{27,30} Here, we revealed that cysteine was the most effective activator of the Pib2-dependent pathway. Further, we showed that cysteine binds to Pib2 via the T motif and determined that the two most critical residues for this binding are W632 and F635. The T motif has been reported to be essential for the Pib2 activation of TORC1.^{26,29} Cysteine binding enhances TORC1 binding via the E domain (residues 304–425); it was previously shown that this domain is the Kog1-binding domain of Pib2 and that it engages

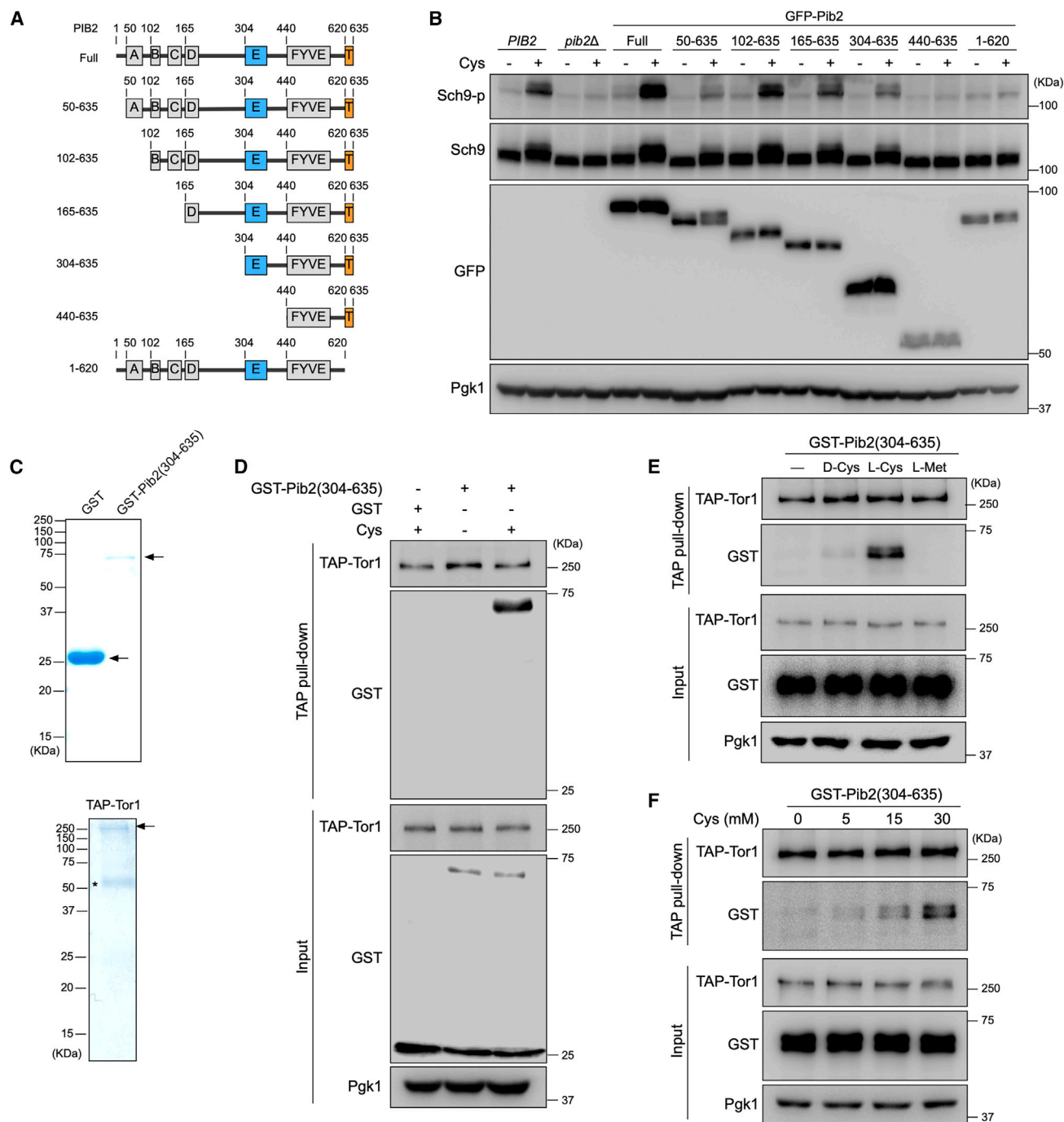


Figure 5. Cysteine promotes Pib2-TORC1 interaction *in vitro*

(A) Schematic diagram of Pib2 with defined motifs and the truncation mutants.

(B) WT cells (BY4741), *pib2Δ* cells (HUY28A), and cells expressing each *pib2* truncation mutant (YAY2569, YAY2575, YAY2570, YAY2571, YAY2572, YAY2573, YAY2574) were nitrogen starved for 30 min, and then 5 mM cysteine was added for 6 min.

(C) GST alone (as control) or GST-Pib2(304–635) was purified from *E. coli*, and TAP alone (as control) or TAP-Tor1 was purified from yeast (ZQZ230, ZQZ231); all were then subjected to SDS-PAGE and stained with CBB. The asterisk indicates non-specific bands.

(D) Lysates from yeast cells (ZQZ230) expressing TAP-tagged Tor1 were immunoprecipitated by IgG-Dynabeads. Beads conjugated to TAP-Tor1 were incubated with purified GST-Pib2(304–635), with or without 30 mM cysteine, for 3 h at 4°C and then subjected to TAP pull-down assay.

(E) TAP pull-down assay with or without 30 mM concentrations of the indicated aa, as in (D).

(F) TAP pull-down assay with the indicated concentrations of L-cysteine, as in (D).

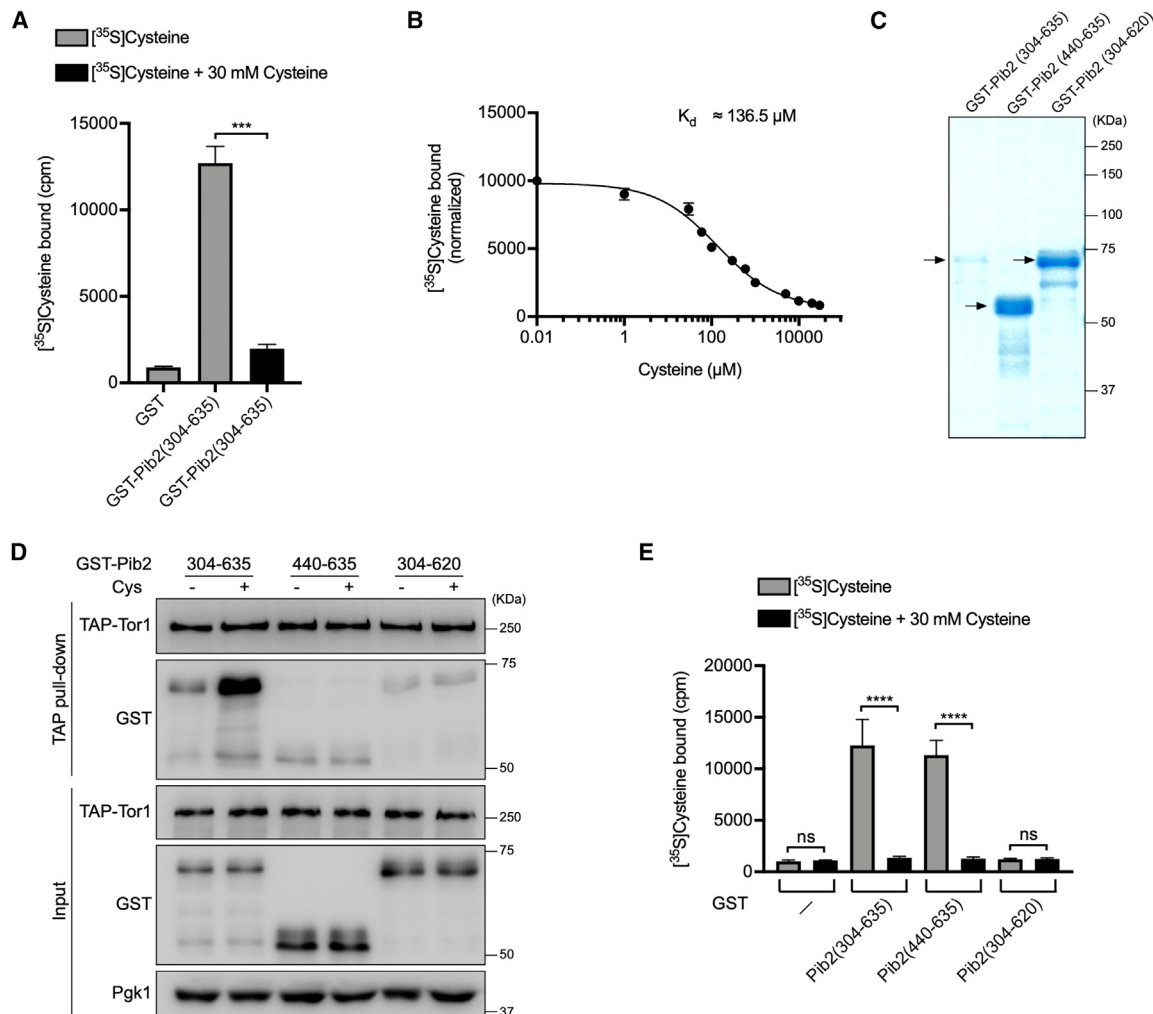


Figure 6. Cysteine directly binds to Pib2

(A) Beads binding GST and GST-Pib2(304–635) were purified from *E. coli* and incubated with 2 μCi L- $[^{35}\text{S}]$ -cysteine, with or without unlabeled cysteine. After washout, the radioactivity of the beads was measured. The values shown are means \pm SD for three technical replicates from one representative experiment. Unpaired t test. **** $p < 0.0001$.

(B) GST-Pib2(304–635) was analyzed in binding assays as in (A), with 2 μCi L- $[^{35}\text{S}]$ -cysteine and the indicated concentrations of unlabeled cysteine. Each point in the graph represents the normalized mean \pm SD for three technical replicates in an assay with 2 μCi L- $[^{35}\text{S}]$ -cysteine. The K_D was calculated from the results of two independent biology replicates, each of which included three technical replicates.

(C and D) GST-tagged Pib2 truncated proteins were prepared and analyzed by SDS-PAGE and CBB staining. TAP pull-down assay was performed as in Figure 5E.

(E) GST-tagged proteins were prepared and cysteine-binding assays were performed and analyzed as in (A). Unpaired t test. ns, no significance, **** $p < 0.0001$.

in Pib2-TORC1 interaction.^{26,28,30} Cysteine binding may shift the Pib2 structure, including the E motif, thereby promoting its interaction with TORC1, though further research is necessary to elucidate the detailed mechanism. D-cysteine, the enantiomer of L-cysteine, did not promote Pib2-TORC1 interaction. Further, TORC1 activation by the other Pib2-binding amino acid, glutamine, was not affected by the loss of the two critical residues W632 and F635, indicating that the structural properties of L-cysteine are crucial for this binding. It was reported that Pib2 plays a crucial role in glutamine sensing, while the binding of glutamine occurs in Pib2 recombinant protein only in combination with additional factors.²⁸ Glutamine affects the folding state of Pib2,

whereas the effect is to be explored.^{28,30} By contrast, this study shows that cysteine binds directly to Pib2 recombinant protein alone *in vitro*, elucidating that Pib2 itself functions as a cysteine sensor.

Although intracellular cysteine concentrations vary depending on numerous factors, such as genetic background and growth conditions, some studies reported concentrations of approximately 80 μM .^{45,46} Our results indicated that TORC1 was minimally activated by adding 50–100 μM cysteine to the medium, and the K_D of Pib2 for cysteine was determined to be 136.5 μM . Pib2 sways due to its intrinsically disordered regions (IDRs), and this movement promotes the dissociation of glutamine,³⁰

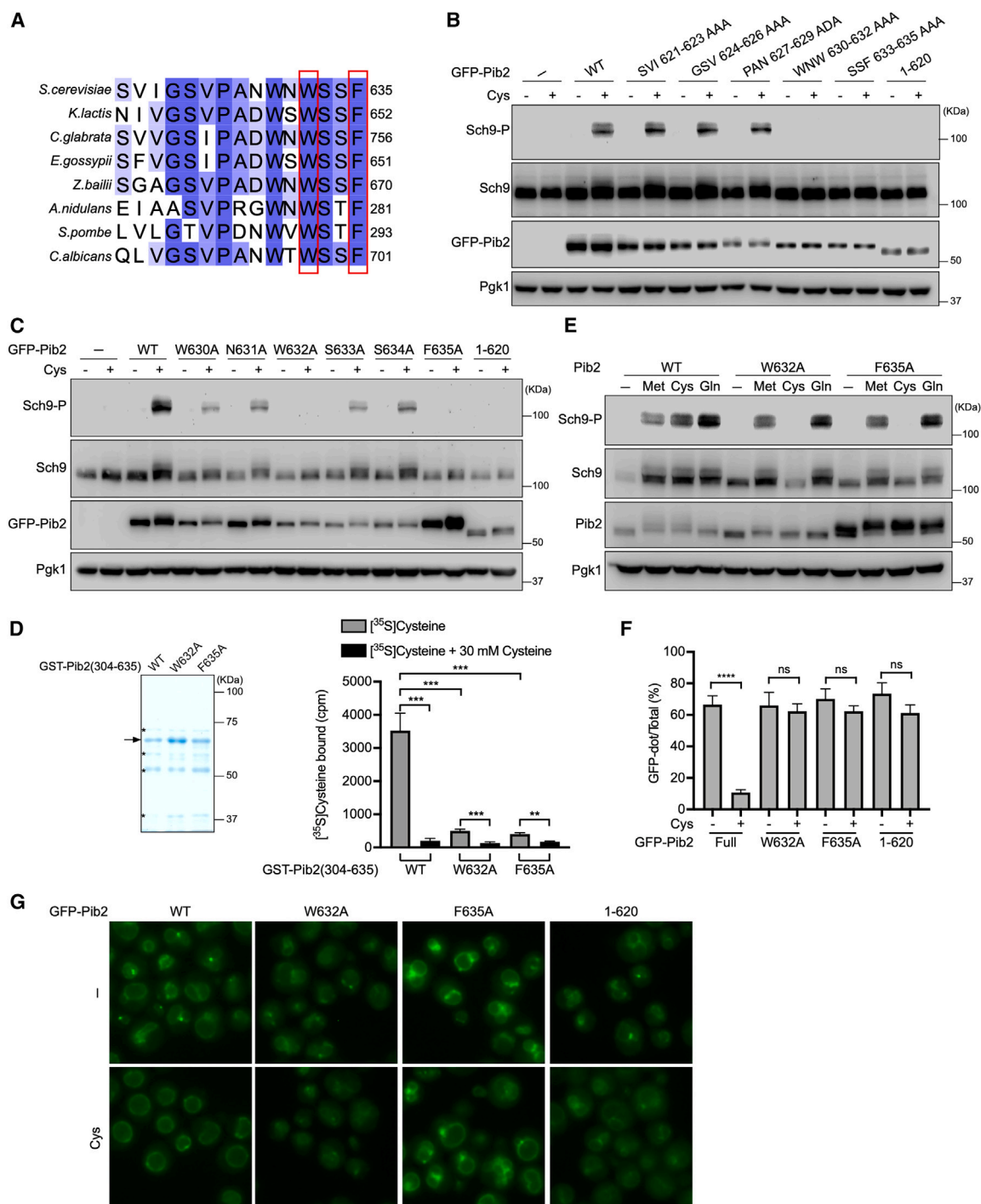


Figure 7. Pib2 W632 and F635 are essential for TORC1 activation by cysteine

(A) Alignment of the T motifs in Pib2 ortholog proteins from various fungal species.
 (B) *pib2Δ* cells (HUY28A) expressing GFP-Pib2 (YAY2569) or each Pib2 T-motif mutant (ZQZ238, ZQZ239, ZQZ240, ZQZ241, ZQZ242) were nitrogen starved for 30 min and then restimulated with or without 5 mM cysteine for 6 min.
 (C) *pib2Δ* cells (HUY28A) expressing GFP-Pib2 (YAY2569) or each Pib2 T-motif mutant (ZQZ253, ZQZ254, ZQZ255, ZQZ256, ZQZ257, ZQZ258, YAY2574) were analyzed as in (B).
 (D) GST-tagged Pib2 truncated proteins were prepared and analyzed by SDS-PAGE and CBB staining. Cysteine-binding assays were performed and analyzed as in Figure 6A. The arrow indicates GST-Pib2, and the asterisks indicate contaminants or degradation products. Unpaired t test. ***p* < 0.01, ****p* < 0.001.
 (E) WT cells (BY4741) or cells with Pib2 mutation W632A (ZQZ264) or F635A (ZQZ265) were analyzed as in (B).
 (F and G) *pib2Δ* cells expressing GFP-Pib2 (YAY2569) or each Pib2 T-motif mutant (ZQZ255, ZQZ258, YAY2574). Cells were cultured as in Figure 2D. Scale bar: 5 μm.
 (F) The graph represent means ± SD (*n* > 70). Unpaired t test. ns, no significance, *****p* < 0.0001.

which might influence cysteine binding. Additional structural studies will provide insight into which properties of cysteine-Pib2 binding enhance the interaction of Pib2 with TORC1.

Cysteine has many metabolic and regulatory roles in yeast cells, not only through its function as a proteinogenic amino acid but also as a precursor for pivotal molecules such as glutathione, taurine, co-enzyme A, and iron-sulfur clusters, all of which play crucial roles in numerous cellular reactions.^{47–49} Therefore, it is reasonable that cysteine levels are monitored by TORC1 activation in response to cellular demands.

Although there are some reports that the absence of either the Pib2 or Gtr pathway prevents phase 1 (acute and transient) TORC1 activation by amino acids,^{26,50} our results suggest that different amino acids exhibit different dependencies on the Gtr and Pib2 pathways in the activation of TORC1. Acute and transient TORC1 activation may be associated with the activation of some phosphatases, although we could not evaluate this issue in this study. Consistent with previous reports, our results indicate that TORC1 activation by leucine^{10,51} and methionine⁵² is more dependent on the Gtr pathway, while activation by glutamine is more dependent on the Pib2 pathway.^{27,28} We could not establish a general rule for the classification of amino acids into each type, even based on their relationship to metabolic pathways or pH in dissolved media (Table S2). Each amino acid also exhibited various dependencies on the Rag pathway in mammals (Figure S6E),⁵³ although at this stage, we cannot identify a general rule regarding the differences. Of note, however, the molecular weights of most type 2 amino acids (Cys [121.2], Gly [75.07], Gln [146.1], Val [117.1], and Ala [89.09]) are smaller than those of type 1 amino acids (Met [149.2], Leu [131.2], Ile [131.2], Glu [147.1], Asp [133.1], His [155.2], Phe [165.2], Tyr [181.2], and Trp [204.2]), which may help clarify this issue in the future.

An important observation is that type 3 amino acids (Lys, Pro, and Arg) were dependent on both the Gtr and Pib2 pathways. Multiple groups, including ours, have proposed that the Gtr and Pib2 pathways act in parallel.^{27–29} However, several reports have suggested a cooperative relationship between the two pathways.^{26,50} Lys and Arg are both basic amino acids that pool abundantly in vacuoles under nutrient-rich conditions and are released into the cytosol during nitrogen starvation.⁵⁴ Proline is categorized as one of the poor amino acids as nitrogen source poorly supporting cellular growth.⁵⁵ It is unclear how these properties fit with our results; however, some sort of functional interaction between the two pathways may exist, at least in response to these amino acids. In addition, all 20 amino acids somehow increased Ser3 phosphorylation in wild-type cells, which may stem from the interactions between the two pathways.

Here, we identified Ser3 as a TORC1 substrate that is dependent on the Pib2 pathway. In addition to well-studied TORC1 substrates such as Sch9, Atg13, Sit4, Sfp1, and Ypk3,^{3,5,56,57} phosphoproteomic studies revealed several other possible TORC1 substrates,⁵⁸ but Ser3 was not among them. Although we did not thoroughly evaluate Ser33 in this study, it behaves similarly to Ser3, so we suggest that both Ser3 and Ser33 are TORC1 substrates. Ser3 and Ser33 are phosphoglycerate dehydrogenases that are involved in serine biosynthesis.³³ It is possible that Pib2-pathway-dependent phosphorylation affects Ser3 func-

tion, especially in terms of its enzymatic activity, and our group is in the process of analyzing this issue. We are now investigating the physiological significance of Ser3 and Ser33 phosphorylation, especially in terms of their enzymatic activity, by analyzing their TORC1-dependent phosphorylation sites in another line of study.

We showed that Ser3 phosphorylation is not dependent on Gtr but is instead wholly dependent on Pib2, indicating that Ser3 is a Pib2-pathway-specific TORC1 substrate. It is an emerging concept that the phosphorylation of each (m)TORC1 substrate does not necessarily represent general activity status. For example, TFEB reacts differently than S6K and 4E-BP1 in response to specific inputs such as amino acids and growth factors.⁵⁹ This diversity stems from the different mechanisms whereby these substrates are recruited to mTORC1 via RagC. In mammals and *Schizosaccharomyces pombe*, some TORC1 substrates contain the TOS motif, by which they are recruited to TORC1 via binding to Raptor.⁶⁰ Meanwhile, the distinct spatial distribution of TORC1 exhibits a diverse mechanism of substrate recruitment. In mammals, mTORC1 receives signals from lysosomes or the Golgi compartment, and the signals preferentially control S6K or 4E-BP, respectively.⁶¹ In yeast, the differential localization of TORC1 on vacuoles or endosomes controls the phosphorylation of Sch9 or Atg13/Vps27.⁶² However, Ser3 is the first identified substrate that is totally dependent on only one TORC1 pathway. Especially in *gtr1Δ* cells, Ser3 is co-localized with TORC1 in vacuole-associated puncta, which, together with MS data in this study, supports a physical association with TORC1 and/or Pib2. Elucidating the recruitment mechanism will help determine in detail why Ser3 depends on the Pib2 pathway.

In conclusion, Pib2 serves as a cysteine sensor for the TORC1 pathway. This study expanded the concept that each amino acid is monitored individually in various organisms in a diverse manner. Cysteine activates mTORC1 in mouse embryonic fibroblast (MEF) cells in a manner dependent on Rag GTPase.^{29,53} LAPF, a possible Pib2 homolog in humans, conserves the FYVE domain of Pib2 but does not affect glutamine-induced mTORC1 activation.⁵³ However, LAPF conserves the T motif of Pib2, including two crucial amino acid residues, W632 and F635.²⁹ In the future, it will be interesting to explore LAPF function in the context of mammalian cysteine sensing and metabolic regulation.

Limitations of the study

One limitation of our study is the lack of a comprehensive structural understanding of cysteine binding. Further investigation is required to gain a more detailed insight into how the structure of Pib2 is influenced by cysteine binding and its subsequent impact on TORC1 activation. Additionally, exploring the effects of other type 2 amino acids in these mechanisms would provide valuable avenues for research.

STAR★METHODS

Detailed methods are provided in the online version of this paper and include the following:

- KEY RESOURCES TABLE
- RESOURCE AVAILABILITY

- Lead contact
- Materials availability
- Data and code availability
- **EXPERIMENTAL MODEL AND SUBJECT PARTICIPANT DETAILS**
- **METHOD DETAILS**
 - Yeast strains, plasmids, and growth conditions
 - Fluorescence microscopy
 - *In vitro* kinase assays
 - Cell lysate preparation and Western blot analysis
 - Immunoprecipitation experiments
 - Protein purification
 - *In vitro* binding assay
 - Cysteine uptake assay
 - Cysteine-binding assay and K_d calculation
 - LC-MS analysis
- **QUANTIFICATION AND STATISTICAL ANALYSIS**

SUPPLEMENTAL INFORMATION

Supplemental information can be found online at <https://doi.org/10.1016/j.celrep.2023.113599>.

ACKNOWLEDGMENTS

We are grateful to Dr. Takayuki Sekito (The University of Ehime) and Dr. Nobuo Noda (The University of Hokkaido) for their scientific discussions that contributed to this study. This study is funded by Grants-in-Aid for Scientific Research (23H02475 and 22H04647 to T.N. and 18K06111 and 21K06170 to Y.A.). This research was also conducted as part of the All-Osaka U Research in "The Nippon Foundation - Osaka University Infectious Disease Response Project."

AUTHOR CONTRIBUTIONS

Conceptualization, T.N., Y.A., and Q.Z.; experimental design, T.N., Y.A., and Q.Z.; methodology, Y.A. and Q.Z.; investigation, Q.Z. and Y.A.; data analysis, Q.Z. and Y.A.; writing – original draft, Q.Z.; writing – review & editing, T.N. and Y.A.; visualization, Q.Z., T.N., and Y.A.; supervision, T.N. and Y.A.; funding acquisition, T.N. and Y.A.

DECLARATION OF INTERESTS

The authors declare no competing interests.

Received: July 11, 2023

Revised: October 24, 2023

Accepted: December 4, 2023

REFERENCES

1. Loewith, R., and Hall, M.N. (2011). Target of rapamycin (TOR) in nutrient signaling and growth control. *Genetics* 189, 1177–1201.
2. Chantranupong, L., Wolfson, R.L., and Sabatini, D.M. (2015). Nutrient-sensing mechanisms across evolution. *Cell* 161, 67–83.
3. Urban, J., Soultard, A., Huber, A., Lippman, S., Mukhopadhyay, D., DeLoche, O., Wanke, V., Anrather, D., Ammerer, G., Riezman, H., et al. (2007). Sch9 is a major target of TORC1 in *Saccharomyces cerevisiae*. *Mol. Cell* 26, 663–674.
4. Jin, N., Mao, K., Jin, Y., Tevzadze, G., Kauffman, E.J., Park, S., Bridges, D., Loewith, R., Saltiel, A.R., Klionsky, D.J., and Weisman, L.S. (2014). Roles for PI(3,5)P₂ in nutrient sensing through TORC1. *Mol. Biol. Cell* 25, 1171–1185.
5. Kamada, Y., Yoshino, K.I., Kondo, C., Kawamata, T., Oshiro, N., Yonezawa, K., and Ohsumi, Y. (2010). Tor directly controls the Atg1 Kinase complex to regulate autophagy. *Mol. Cell Biol.* 30, 1049–1058.
6. Noda, T., and Ohsumi, Y. (1998). Tor, a phosphatidylinositol kinase homologue, controls autophagy in yeast. *J. Biol. Chem.* 273, 3963–3966.
7. Suzuki, H., Osawa, T., Fujioka, Y., and Noda, N.N. (2017). Structural biology of the core autophagy machinery. *Curr. Opin. Struct. Biol.* 43, 10–17.
8. Suzuki, K., and Ohsumi, Y. (2010). Current knowledge of the pre-autophagosomal structure (PAS). *FEBS Lett.* 584, 1280–1286.
9. Fujioka, Y., Alam, J.M., Noshiro, D., Mouri, K., Ando, T., Okada, Y., May, A.I., Knorr, R.L., Suzuki, K., Ohsumi, Y., and Noda, N.N. (2020). Phase separation organizes the site of autophagosome formation. *Nature* 578, 301–305.
10. Binda, M., Péli-Gulli, M.P., Bonfils, G., Panchaud, N., Urban, J., Sturgill, T.W., Loewith, R., and De Virgilio, C. (2009). The Vam6 GEF controls TORC1 by activating the EGO Complex. *Mol. Cell* 35, 563–573.
11. Sancak, Y., Peterson, T.R., Shaul, Y.D., Lindquist, R.A., Thoreen, C.C., Bar-Peled, L., and Sabatini, D.M. (2008). The Rag GTPases bind raptor and mediate amino acid signaling to mTORC1. *Science* 320, 1496–1501.
12. Sancak, Y., Bar-Peled, L., Zoncu, R., Markhard, A.L., Nada, S., and Sabatini, D.M. (2010). Regulator-Rag complex targets mTORC1 to the lysosomal surface and is necessary for its activation by amino acids. *Cell* 141, 290–303.
13. Jewell, J.L., Russell, R.C., and Guan, K.-L. (2013). Amino acid signalling upstream of mTOR. *Nat. Rev. Mol. Cell Biol.* 14, 133–139.
14. Bar-Peled, L., Chantranupong, L., Cherniack, A.D., Chen, W.W., Ottina, K.A., Grabiner, B.C., Spear, E.D., Carter, S.L., Meyerson, M., and Sabatini, D.M. (2013). A Tumor suppressor complex with GAP activity for the Rag GTPases That signal amino acid sufficiency to mTORC1. *Science* 340, 1100–1106.
15. Condon, K.J., and Sabatini, D.M. (2019). Nutrient regulation of mTORC1 at a glance. *J. Cell Sci.* 132, jcs222570.
16. Powis, K., Zhang, T., Panchaud, N., Wang, R., De Virgilio, C., and Ding, J. (2015). Crystal structure of the Ego1-Ego2-Ego3 complex and its role in promoting Rag GTPase-dependent TORC1 signaling. *Cell Res.* 25, 1043–1059.
17. Panchaud, N., Péli-Gulli, M.P., and De Virgilio, C. (2013). Amino acid deprivation inhibits TORC1 through a GTPase-activating protein complex for the Rag family GTPase Gtr1. *Sci. Signal.* 6, ra42.
18. Panchaud, N., Péli-Gulli, M.P., and De Virgilio, C. (2013). SEACing the GAP that nEGOCiates TORC1 activation: Evolutionary conservation of Rag GTPase regulation. *Cell Cycle* 12, 2948–2952.
19. Nicastro, R., Sardu, A., Panchaud, N., and De Virgilio, C. (2017). The Architecture of the Rag GTPase Signaling Network. *Biomolecules* 7, 48.
20. Kira, S., Tabata, K., Shirahama-Noda, K., Nozoe, A., Yoshimori, T., and Noda, T. (2014). Reciprocal conversion of Gtr1 and Gtr2 nucleotide-binding states by Npr2-Npr3 inactivates TORC1 and induces autophagy. *Autophagy* 10, 1565–1578.
21. Kira, S., Kumano, Y., Ukai, H., Takeda, E., Matsuura, A., and Noda, T. (2016). Dynamic relocation of the TORC1–Gtr1/2–Ego1/2/3 complex is regulated by Gtr1 and Gtr2. *Mol. Biol. Cell* 27, 382–396.
22. Wolfson, R.L., Chantranupong, L., Saxton, R.A., Shen, K., Scaria, S.M., Cantor, J.R., and Sabatini, D.M. (2016). Sestrin2 is a leucine sensor for the mTORC1 pathway. *Science* 351, 43–48.
23. Chantranupong, L., Scaria, S.M., Saxton, R.A., Gygi, M.P., Shen, K., Wyant, G.A., Wang, T., Harper, J.W., Gygi, S.P., and Sabatini, D.M. (2016). The CASTOR Proteins Are Arginine Sensors for the mTORC1 Pathway. *Cell* 165, 153–164.
24. Gu, X., Orozco, J.M., Saxton, R.A., Condon, K.J., Liu, G.Y., Krawczyk, P.A., Scaria, S.M., Harper, J.W., Gygi, S.P., and Sabatini, D.M. (2017). SAMTOR is an S-adenosylmethionine sensor for the mTORC1 pathway. *Science* 358, 813–818.

25. Chen, J., Ou, Y., Luo, R., Wang, J., Wang, D., Guan, J., Li, Y., Xia, P., Chen, P.R., and Liu, Y. (2021). SAR1B senses leucine levels to regulate mTORC1 signalling. *Nature* 596, 281–284.
26. Michel, A.H., Hatakeyama, R., Kimmig, P., Arter, M., Peter, M., Matos, J., De Virgilio, C., and Kornmann, B. (2017). Functional mapping of yeast genomes by saturated transposition. *Elife* 6, e23570.
27. Tanigawa, M., and Maeda, T. (2017). An *In Vitro* TORC1 Kinase Assay That Recapitulates the Gtr-Independent Glutamine-Responsive TORC1 Activation Mechanism on Yeast Vacuoles. *Mol. Cell Biol.* 37, e00075-17.
28. Ukai, H., Araki, Y., Kira, S., Oikawa, Y., May, A.I., and Noda, T. (2018). Gtr/Ego-independent TORC1 activation is achieved through a glutamine-sensitive interaction with Pib2 on the vacuolar membrane. *PLoS Genet.* 14, e1007334.
29. Kim, A., and Cunningham, K.W. (2015). A LAPF/phafin1-like protein regulates TORC1 and lysosomal membrane permeabilization in response to endoplasmic reticulum membrane stress. *Mol. Biol. Cell* 26, 4631–4645.
30. Tanigawa, M., Yamamoto, K., Nagatoishi, S., Nagata, K., Noshiro, D., Noda, N.N., Tsumoto, K., and Maeda, T. (2021). A glutamine sensor that directly activates TORC1. *Commun. Biol.* 4, 1093.
31. Hatakeyama, R. (2021). Pib2 as an Emerging Master Regulator of Yeast TORC1. *Biomolecules* 11, 1489.
32. Wallace, R.L., Lu, E., Luo, X., and Capaldi, A.P. (2022). Ait1 regulates TORC1 signaling and localization in budding yeast. *Elife* 11, e68773.
33. Albers, E., Laizé, V., Blomberg, A., Hohmann, S., and Gustafsson, L. (2003). Ser3p (Yer081wp) and Ser33p (Yil074cp) Are Phosphoglycerate Dehydrogenases in *Saccharomyces cerevisiae*. *J. Biol. Chem.* 278, 10264–10272.
34. Mudholkar, K., Fitzke, E., Prinz, C., Mayer, M.P., and Rospert, S. (2017). The Hsp70 homolog Ssb affects ribosome biogenesis via the TORC1-Sch9 signaling pathway. *Nat. Commun.* 8, 937.
35. Heitman, J., Movva, N.R., and Hall, M.N. (1991). Targets for cell cycle arrest by the immunosuppressant rapamycin in yeast. *Science* 253, 905–909.
36. Mülleder, M., Capuano, F., Pir, P., Christen, S., Sauer, U., Oliver, S.G., and Ralser, M. (2012). A prototrophic deletion mutant collection for yeast metabolomics and systems biology. *Nat. Biotechnol.* 30, 1176–1178.
37. Reidman, S., Cohen, A., Kupiec, M., and Weisman, R. (2019). The cytosolic form of aspartate aminotransferase is required for full activation of TOR complex 1 in fission yeast. *J. Biol. Chem.* 294, 18244–18255.
38. Noda, T. (2017). Regulation of Autophagy through TORC1 and mTORC1. *Biomolecules* 7, 52.
39. Kotani, T., Kirisako, H., Koizumi, M., Ohsumi, Y., and Nakatogawa, H. (2018). The Atg2-Atg18 complex tethers pre-autophagosomal membranes to the endoplasmic reticulum for autophagosome formation. *Proc. Natl. Acad. Sci. USA* 115, 10363–10368.
40. Merhi, A., and André, B. (2012). Internal amino acids promote Gap1 permease ubiquitylation via TORC1/Npr1/14-3-3-dependent control of the Bul arrestin-like adaptors. *Mol. Cell Biol.* 32, 4510–4522.
41. Bianchi, F., Van'T Klooster, J.S., Ruiz, S.J., and Poolman, B. (2019). Regulation of Amino Acid Transport in *Saccharomyces cerevisiae*. *Microbiol. Mol. Biol. Rev.* 83, e00024-19.
42. Kaur, J., and Bachhawat, A.K. (2007). Yct1p, a novel, high-affinity, cysteine-specific transporter from the yeast *Saccharomyces cerevisiae*. *Genetics* 176, 877–890.
43. Düring-Olsen, L., Regenbreg, B., Gjermansen, C., Kielland-Brandt, M.C., and Hansen, J. (1999). Cysteine uptake by *Saccharomyces cerevisiae* is accomplished by multiple permeases. *Curr. Genet.* 35, 609–617.
44. Wu, A.L., and Moye-Rowley, W.S. (1994). GSH1, which encodes gamma-glutamylcysteine synthetase, is a target gene for yAP-1 transcriptional regulation. *Mol. Cell Biol.* 14, 5832–5839.
45. Kitamoto, K., Yoshizawa, K., Ohsumi, Y., and Anraku, Y. (1988). Dynamic aspects of vacuolar and cytosolic amino acid pools of *Saccharomyces cerevisiae*. *J. Bacteriol.* 170, 2683–2686.
46. Kitajima, T., Jigami, Y., and Chiba, Y. (2012). Cytotoxic Mechanism of Selenomethionine in Yeast. *J. Biol. Chem.* 287, 10032–10038.
47. Paul, B.D., Sbodio, J.I., and Snyder, S.H. (2018). Cysteine Metabolism in Neuronal Redox Homeostasis. *Trends Pharmacol. Sci.* 39, 513–524.
48. Yin, J., Ren, W., Yang, G., Duan, J., Huang, X., Fang, R., Li, C., Li, T., Yin, Y., Hou, Y., et al. (2016). L-Cysteine metabolism and its nutritional implications. *Mol. Nutr. Food Res.* 60, 134–146.
49. Thomas, D., and Surdin-Kerjan, Y. (1997). Metabolism of sulfur amino acids in *Saccharomyces cerevisiae*. *Microbiol. Mol. Biol. Rev.* 61, 503–532.
50. Varlakhanova, N.V., Mihalevic, M., Bernstein, K.A., and Ford, M.G.J. (2017). Pib2 and EGO Complex are both required for activation of TORC1. *J. Cell Sci.* 207970.
51. Bonfils, G., Jaquenoud, M., Bontron, S., Ostrowicz, C., Ungermann, C., and De Virgilio, C. (2012). Leucyl-tRNA Synthetase Controls TORC1 via the EGO Complex. *Mol. Cell* 46, 105–110.
52. Sutter, B.M., Wu, X., Laxman, S., and Tu, B.P. (2013). Methionine Inhibits Autophagy and Promotes Growth by Inducing the SAM-Responsive Methylation of PP2A. *Cell* 154, 403–415.
53. Meng, D., Yang, Q., Wang, H., Melick, C.H., Naviani, R., Frank, A.R., and Jewell, J.L. (2020). Glutamine and asparagine activate mTORC1 independently of Rag GTPases. *J. Biol. Chem.* 295, 2890–2899.
54. Kawano-Kawada, M., Kakinuma, Y., and Sekito, T. (2018). Transport of Amino Acids across the Vacuolar Membrane of Yeast: Its Mechanism and Physiological Role. *Biol. Pharm. Bull.* 41, 1496–1501.
55. Stracka, D., Jozefczuk, S., Rudroff, F., Sauer, U., and Hall, M.N. (2014). Nitrogen source activates TOR (target of rapamycin) complex 1 via glutamine and independently of Gtr/Rag proteins. *J. Biol. Chem.* 289, 25010–25020.
56. Lempiäinen, H., Uotila, A., Urban, J., Dohnal, I., Ammerer, G., Loewith, R., and Shore, D. (2009). Sfp1 interaction with TORC1 and Mrs6 reveals feedback regulation on TOR signaling. *Mol. Cell* 33, 704–716.
57. Yerlikaya, S., Meusburger, M., Kumari, R., Huber, A., Anrather, D., Costanzo, M., Boone, C., Ammerer, G., Baranov, P.V., and Loewith, R. (2016). TORC1 and TORC2 work together to regulate ribosomal protein S6 phosphorylation in *Saccharomyces cerevisiae*. *Mol. Biol. Cell* 27, 397–409.
58. Dokládál, L., Stumpe, M., Hu, Z., Jaquenoud, M., Dengjel, J., and De Virgilio, C. (2021). Phosphoproteomic responses of TORC1 target kinases reveal discrete and convergent mechanisms that orchestrate the quiescence program in yeast. *Cell Rep.* 37, 110149.
59. Napolitano, G., Di Malta, C., Esposito, A., De Araujo, M.E.G., Pece, S., Bertalot, G., Matarese, M., Benedetti, V., Zampelli, A., Stasyk, T., et al. (2020). A substrate-specific mTORC1 pathway underlies Birt-Hogg-Dubé syndrome. *Nature* 585, 597–602.
60. Morozumi, Y., Hishinuma, A., Furusawa, S., Sofyantor, F., Tatebe, H., and Shiozaki, K. (2021). Fission yeast TOR complex 1 phosphorylates Psk1 through an evolutionarily conserved interaction mediated by the TOS motif. *J. Cell Sci.* 134, jcs258865.
61. Fan, S.-J., Snell, C., Turley, H., Li, J.-L., McCormick, R., Perera, S.M.W., Heublein, S., Kazi, S., Azad, A., Wilson, C., et al. (2016). PAT4 levels control amino-acid sensitivity of rapamycin-resistant mTORC1 from the Golgi and affect clinical outcome in colorectal cancer. *Oncogene* 35, 3004–3015.
62. Hatakeyama, R., Péli-Gulli, M.P., Hu, Z., Jaquenoud, M., Garcia Osuna, G.M., Sardu, A., Dengjel, J., and De Virgilio, C. (2019). Spatially Distinct Pools of TORC1 Balance Protein Homeostasis. *Mol. Cell* 73, 325–338.e8.
63. Janke, C., Magiera, M.M., Rathfelder, N., Taxis, C., Reber, S., Maekawa, H., Moreno-Borchart, A., Doenges, G., Schwob, E., Schiebel, E., and Knop, M. (2004). A versatile toolbox for PCR-based tagging of yeast

- genes: new fluorescent proteins, more markers and promoter substitution cassettes. *Yeast* **21**, 947–962.
64. Storici, F., and Resnick, M.A. (2006). The Delitto Perfetto Approach to In Vivo Site-Directed Mutagenesis and Chromosome Rearrangements with Synthetic Oligonucleotides in Yeast. In *Methods in Enzymology* (Elsevier), pp. 329–345.
65. Kaiser, C., Michaelis, S., Mitchell, A., and Laboratory, C.S.H. (1994). *Methods in Yeast Genetics: A Cold Spring Harbor Laboratory Course Manual* (Cold Spring Harbor Laboratory Press).
66. Cools, M., Rompf, M., Mayer, A., and André, B. (2019). Measuring the Activity of Plasma Membrane and Vacuolar Transporters in Yeast. In *Yeast Systems Biology Methods in Molecular Biology*, S.G. Oliver and J.I. Cast-rillo, eds. (Springer New York), pp. 247–261.
67. Ishihama, Y., Oda, Y., Tabata, T., Sato, T., Nagasu, T., Rappsilber, J., and Mann, M. (2005). Exponentially Modified Protein Abundance Index (em-PAI) for Estimation of Absolute Protein Amount in Proteomics by the Number of Sequenced Peptides per Protein. *Mol. Cell. Proteomics* **4**, 1265–1272.

STAR★METHODS

KEY RESOURCES TABLE

REAGENT or RESOURCE	SOURCE	IDENTIFIER
Antibodies		
Mouse monoclonal anti-PGK1 antibody	Thermo Fisher	459250; RRID: AB_2532235
Mouse monoclonal anti-GFP antibody	Roche	11814460001; RRID:AB_390913
Goat polyclonal anti-Tor1 (yN-15) antibody	Santa Cruz	sc-11900; RRID: AB_672897
Rat monoclonal anti-HA antibody	Roche	11867423001; RRID:AB_390918
anti-Sch9 antibody	Lab stock	N/A
anti-phospho-Sch9-T737 antibody	Lab stock	N/A
anti-Pib2 antibody	Lab stock	N/A
anti-GST antibody	Lab stock	N/A
HRP-conjugated goat anti-mouse IgG antibody	Jackson ImmunoResearch	115-035-003; RRID:AB_10015289
HRP-conjugated goat anti-rabbit IgG antibody	Jackson ImmunoResearch	111-035-003; RRID:AB_2313567
HRP-conjugated goat anti-rat IgG antibody	Cell Signaling Technology	7077; RRID:AB_10694715
HRP-conjugated rabbit anti-goat IgG antibody (anti-TAP)	Abcam	ab6741; RRID:AB_955424
Bacterial and virus strains		
<i>E. coli</i> DH5 α	BioElegen Technology	DH01-20
<i>E. coli</i> Rosetta 2 (DE3)	Novagen	71397
Chemicals, peptides, and recombinant proteins		
Rapamycin	LKT Laboratories	53123-88-9
Cycloheximide	Nacalai tesque	66-81-9
Yeast extract	BD Biosciences	212750
Peptone	BD Biosciences	211677
Glucose	Wako	50-99-7
Yeast nitrogen base without amino acids and ammonium sulfate	BD Biosciences	DF0335-15-9
Ammonium sulfate	Nacalai tesque	7783-20-2
Casamino acid	BD Biosciences	223050
Trichloroacetic acid	Wako	76-03-9
Triton X-100	Wako	9002-93-1
Ethanol	Nacalai tesque	64-17-5
Urea	Wako	57-13-6
SDS	Nacalai tesque	151-21-3
EDTA	Sigma-Aldrich	60-00-4
Tris	Nacalai tesque	77-86-1
NaCl	Wako	7647-14-5
Imidazole	Wako	288-32-4
HEPES	Sigma-Aldrich	7365-45-9
Phos-tag	Wako	AAL-107
ATP Solution	Thermo Fisher	R0441
MnCl ₂	Sigma-Aldrich	7773-01-5
DTT	Wako	3483-12-3
PMSF	Wako	329-98-6

(Continued on next page)

Continued

REAGENT or RESOURCE	SOURCE	IDENTIFIER
PhosSTOP	Roche	4906837001
Complete EDTA-free protease inhibitor cocktail	Roche	11873580001
Ni-NTA beads	QIAGEN	30210
GST-Accept	Nacalai tesque	09277-56
IPTG (Isopropyl- β -D-thiogalactoside)	TAKARA	9030
DMSO	Sigma-Aldrich	67-68-5
Sodium phosphate	Wako	7558-79-4
β -Mercaptoethanol	Wako	60-24-2
Bromophenol blue	Sigma-Aldrich	115-39-9
IgG coupled to Dynabeads (M-270 Epoxy)	Thermo Fisher	14301
ChromoTek GFP-Trap Magnetic Agarose	Proteintech	gtma-100; RRID:AB_2631358
Chloramphenicol	Wako	56-75-7
Glutathione Sepharose beads	Nacalai tesque	09277-56
Reduced glutathione	Wako	70-18-8
L-[35 S]-cysteine	PerkinElmer	NEG022T
Scintillation fluid	Nacalai tesque	09135-51
Coomassie brilliant blue	Wako	6104-59-2
L-Glycine	Wako	56-40-6
L-Alanine	Sigma-Aldrich	56-41-7
L-Serine	Sigma-Aldrich	56-45-1
L-Proline	Wako	147-85-3
L-Valine	Wako	72-18-4
L-Threonine	Sigma-Aldrich	72-19-5
L-Cysteine	Wako	52-90-4
L-Leucine	Sigma-Aldrich	61-90-5
L-Isoleucine	Sigma-Aldrich	73-32-5
L-Aspartate	Sigma-Aldrich	56-84-8
L-Glutamine	Wako	56-85-9
L-Lysine	Sigma-Aldrich	657-27-2
L-Glutamate	Sigma-Aldrich	142-49-2
L-Methionine	Wako	63-68-3
L-Histidine	Sigma-Aldrich	71-00-1
L-Phenylalanine	Sigma-Aldrich	63-91-2
L-Arginine	Wako	74-79-3
L-Tyrosine	Sigma-Aldrich	60-18-4
L-Tryptophan	Sigma-Aldrich	73-22-3
D-cysteine	Combi-Blocks	32443-99-5
Critical commercial assays		
Chemi-Lumi One Ultra	Nacalai tesque	11644-40
KOD One PCR Master Mix	TOYOBO	KMM-101
Protein Assay BCA kit	Nacalai tesque	06385-00
Deposited data		
Original data	This study	
Experimental models: Organisms/strains		
BY4741	Brachmann et al., 1998 ⁶³	<i>MATa his3Δ1 leu2Δ0 met15Δ0 ura3Δ0</i>

(Continued on next page)

Continued

REAGENT or RESOURCE	SOURCE	IDENTIFIER
BY4742	Brachmann et al., 1998 ⁶³	<i>MATα. his3Δ1 leu2Δ0 lys2Δ0 ura3Δ0</i>
YAY2674	This study	[BY4742] <i>VPH1-mCherry-hphNT1 gtr1Δ::zeoNT3 SER3-yeGFP-kanMX4</i>
YAY2679	This study	[BY4742] <i>VPH1-mCherry-hphNT1 gtr1Δ::zeoNT3 SER3-yeGFP-kanMX4</i>
YAY2838-1	This study	[BY4741] <i>GFP-TOR1^{11954S}-LEU2</i>
YAY3071	This study	[BY4741] <i>TCO89-mCherry-hphNT1 SER3-yeGFP-kanMX4 gtr1Δ::natNT2</i>
YAY3072	This study	[BY4741] <i>TCO89-mCherry-hphNT1 SER3-yeGFP-kanMX4 gtr1Δ::natNT2</i>
YAY2864	This study	[BY4741] <i>SER3-3HA-kanMX4 pHLUM</i>
YAY2867	This study	[BY4741] <i>SER3-3HA-kanMX4 pHLUM gtr1Δ::hphNT1</i>
YAY2868	This study	[BY4741] <i>SER3-3HA-kanMX4 pHLUM pib2Δ::natNT2</i>
ZQZ108	This study	[BY4741] <i>gtr1Δ::natNT2 ego1Δ::zeoNT3 pHLUM</i>
ZQZ109	This study and Ukai et al., 2018 ²⁸	[BY4741] <i>gtr1Δ::natNT2 ego1Δ::zeoNT3 pHLUM pib2-2-kanMX4</i>
ZQZ101	This study	[BY4741] <i>GFP-TOR1-LEU2 VPH1-mCherry-hphNT1 pHLUM</i>
ZQZ102	This study	[BY4741] <i>GFP-TOR1-LEU2 VPH1-mCherry-hphNT1 pHLUM gtr1Δ::natNT2</i>
ZQZ103	This study	[BY4741] <i>GFP-TOR1-LEU2 VPH1-mCherry-hphNT1 pHLUM pib2Δ::natNT2</i>
ZQZ148	This study	[BY4741] <i>VPH1-mCherry-hphNT1 ATG2-yeGFP-kanMX4</i>
ZQZ150	This study	[BY4741] <i>VPH1-mCherry-hphNT1 ATG2-yeGFP-kanMX4 gtr1Δ::zeoNT3</i>
ZQZ152	This study	[BY4741] <i>VPH1-mCherry-hphNT1 ATG2-yeGFP-kanMX4 pib2Δ::natNT2</i>
ZQZ232	This study	[BY4741] <i>gap1Δ::kanMX6 pHLUM</i>
ZQZ233	This study	[BY4741] <i>yc1Δ::kanMX6 pHLUM</i>
ZQZ114	This study	[BY4741] <i>yeGFP-PIB2 gtr1Δ::natNT2 pHLUM</i>
ZQZ118	This study	[BY4741] <i>SER3-3HA-kanMX4 pHLUM gtr1Δ::hphNT1 gsh1Δ::zeoNT3</i>
ZQZ137	This study	[BY4741] <i>VPH1-mCherry-hphNT1 GAP1-yeGFP-kanMX4</i>
ZQZ138	This study	[BY4741] <i>VPH1-mCherry-hphNT1 GAP1-yeGFP-kanMX4 pib2Δ::natNT2</i>
ZQZ146	This study	[BY4741] <i>VPH1-mCherry-hphNT1 YCT1-yeGFP-kanMX4</i>
ZQZ147	This study	[BY4741] <i>VPH1-mCherry-hphNT1 YCT1-yeGFP-kanMX4 pib2Δ::natNT2</i>
ZQZ116	This study	[BY4741] <i>yeGFP-PIB2 GTR1-TAP::kanMX4 pHLUM</i>
YAY2569	Ukai et al., 2018 ²⁸	[BY4741] <i>pib2Δ::zeoNT3 GFP-PIB2^{full}-kanMX4</i>
YAY2575	Ukai et al., 2018 ²⁸	[BY4741] <i>pib2Δ::zeoNT3 GFP-PIB2⁵⁰⁻⁶³⁵-kanMX4</i>
YAY2570	Ukai et al., 2018 ²⁸	[BY4741] <i>pib2Δ::zeoNT3 GFP-PIB2¹⁰²⁻⁶³⁵-kanMX4</i>
YAY2571	Ukai et al., 2018 ²⁸	[BY4741] <i>pib2Δ::zeoNT3 GFP-PIB2¹⁶⁵⁻⁶³⁵-kanMX4</i>
YAY2572	Ukai et al., 2018 ²⁸	[BY4741] <i>pib2Δ::zeoNT3 GFP-PIB2³⁰⁴⁻⁶³⁵-kanMX4</i>
YAY2573	Ukai et al., 2018 ²⁸	[BY4741] <i>pib2Δ::zeoNT3 GFP-PIB2⁴⁴⁰⁻⁶³⁵-kanMX4</i>
YAY2574	Ukai et al., 2018 ²⁸	[BY4741] <i>pib2Δ::zeoNT3 GFP-PIB2¹⁻⁶²⁰-kanMX4</i>
ZQZ230	This study	[BY4741] <i>TAP-TOR1-LEU2 pib2Δ::natNT2</i>
ZQZ231	This study	[BY4741] <i>pACT1-TAP-NAT-leu2d0-int pib2Δ::natNT2</i>
HUY28A	This study	[BY4741] <i>pib2Δ::zeoNT3</i>
ZQZ238	This study	[BY4741] <i>pib2Δ::zeoNT3 GFP-PIB2^{S621A V622A I623A}-kanMX4</i>
ZQZ239	This study	[BY4741] <i>pib2Δ::zeoNT3 GFP-PIB2^{G624A S625A V626A}-kanMX4</i>

(Continued on next page)

Continued

REAGENT or RESOURCE	SOURCE	IDENTIFIER
ZQZ240	This study	[BY4741] <i>pib2Δ::zeoNT3 GFP-PIB2^{P627A A628D N629A}-kanMX4</i>
ZQZ241	This study	[BY4741] <i>pib2Δ::zeoNT3 GFP-PIB2^{W630A N631A W632A}-kanMX4</i>
ZQZ242	This study	[BY4741] <i>pib2Δ::zeoNT3 GFP-PIB2^{S633A S634A F635A}-kanMX4</i>
ZQZ253	This study	[BY4741] <i>pib2Δ::zeoNT3 GFP-PIB2^{W630A}-kanMX4</i>
ZQZ254	This study	[BY4741] <i>pib2Δ::zeoNT3 GFP-PIB2^{N631A}-kanMX4</i>
ZQZ255	This study	[BY4741] <i>pib2Δ::zeoNT3 GFP-PIB2^{W632A}-kanMX4</i>
ZQZ256	This study	[BY4741] <i>pib2Δ::zeoNT3 GFP-PIB2^{S633A}-kanMX4</i>
ZQZ257	This study	[BY4741] <i>pib2Δ::zeoNT3 GFP-PIB2^{S634A}-kanMX4</i>
ZQZ258	This study	[BY4741] <i>pib2Δ::zeoNT3 GFP-PIB2^{F635A}-kanMX4</i>
ZQZ264	This study	[BY4741] <i>pib2Δ::zeoNT3 PIB2^{W632A}-kanMX4</i>
ZQZ265	This study	[BY4741] <i>pib2Δ::zeoNT3 PIB2^{F635A}-kanMX4</i>

Recombinant DNA

pHLUM	Mülleeder et al., 2012 ³⁵	<i>LEU2, URA3, HIS3, MET15/17</i>
pYA1112	This study	<i>pACT1-TAP-NAT-leu2d0-int</i>
pYA1340	This study	<i>pET28a-SER3</i>
pGEX-6P1-PIB2 ^{304–635}	This study	[pGEX-6P-1(+)] <i>GST-PIB2^{304–635}</i>
pGEX-6P1-PIB2 ^{440–635}	This study	[pGEX-6P-1(+)] <i>GST-PIB2^{440–635}</i>
pGEX-6P1-PIB2 ^{304–620}	This study	[pGEX-6P-1(+)] <i>GST-PIB2^{304–620}</i>
pGEX-6P1-PIB2 ^{304–635 (W632A)}	This study	[pGEX-6P-1(+)] <i>GST-PIB2^{304–635 (W632A)}</i>
pGEX-6P1-PIB2 ^{304–635 (F635A)}	This study	[pGEX-6P-1(+)] <i>GST-PIB2^{304–635 (F635A)}</i>
pRS316	Sikorski and Hieter, 1989 ⁶⁴	<i>CEN, URA3</i>
pSK114	Kira et al., 2016 ²¹	[pRS316] <i>GTR1</i>

Software and algorithms

ImageJ	NIH	https://ImageJ.nih.gov/ij/
Photoshop	Adobe	https://www.adobe.com
Jalview	Waterhouse et al., 2009 ⁶⁵	https://www.jalview.org/
Graphic	Picta Inc	https://www.graphic.com/
GraphPad Prism	GraphPad Software	https://www.graphpad.com/

RESOURCE AVAILABILITY

Lead contact

Further information and requests for resources and reagents should be directed to and will be fulfilled by the lead contact, Takeshi NODA (noda.takeshi.dent@osaka-u.ac.jp).

Materials availability

Plasmids generated in this study are available upon reasonable request.

Data and code availability

- All data reported in this paper will be shared by the [lead contact](#) upon request.
- This paper does not report original code.
- Any additional information required to reanalyze the data reported in this paper is available from the [lead contact](#) upon request.

EXPERIMENTAL MODEL AND SUBJECT PARTICIPANT DETAILS

S. cerevisiae strains are listed in the [Key Resources Table](#). They were grown as described in the [Method Details](#). Recombinant proteins, including GST-PIB2^{304–635}, GST-PIB2^{440–635}, GST-PIB2^{304–620}, GST-PIB2^{304–635 (W632A)}, and GST-PIB2^{304–635 (F635A)}, were expressed in *E. coli* Rosetta 2 (DE3), and cloning procedures were conducted in *E. coli* DH5α.

METHOD DETAILS

Yeast strains, plasmids, and growth conditions

S. cerevisiae strains and plasmids used in this study are listed in the [Key Resources Table](#). Strain construction, gene deletion, and chromosomal epitope tagging were performed as previously reported.^{63,64} Plasmid amplifications were performed using *E. coli* DH5 α , and plasmid sequences were verified by Sanger sequencing (GeneWiz). Yeast cells were grown to mid-log phase in YPD medium (1% yeast extract, 2% peptone, and 2% glucose), SCD medium (0.17% yeast nitrogen base without amino acids or ammonium sulfate, 0.5% ammonium sulfate, 0.5% casamino acid, 2% glucose), or SD-N medium (0.17% yeast nitrogen base without amino acids and ammonium sulfate, 2% glucose). Unless otherwise indicated, yeast cells were cultured at 30°C. Rapamycin was added to medium at a final concentration of 0.2 μ g/mL using a stock solution (1 mg/mL in ethanol and Triton X-100 at a ratio of 9:1 (v/v)). Cycloheximide was added to the medium at a final concentration of 25 μ g/mL using a stock solution (50 mg/mL in DMSO). Each amino acid was added to the medium at a concentration of 5 mM from freshly prepared 50-fold stock solution in medium unless otherwise indicated. Leucine was prepared as a 20-fold stock solution. Complete amino acids were prepared by dissolving a 2% drop-out mixture in the medium.⁶⁵

Fluorescence microscopy

Cells were grown in SCD medium and then shifted to SD-N medium for 30 min of nitrogen starvation, and the indicated amino acids were added. Cells were collected by centrifugation (600 \times g, 2 min) and subjected to microscopy. Cells were observed using a Leica AF6500 fluorescence imaging system (Leica Microsystems) mounted on a DMI6000B microscope (HCX PL APO 100/1.40–0.70 oil-immersion objective lens, xenon lamp (Leica Microsystems)) under the control of LAS-AF software (Leica Microsystems). ImageJ software was used to process images.

In vitro kinase assays

6His-fused Ser3 proteins were expressed in *E. coli* Rosetta 2 (DE3) by adding 0.25 mM isopropyl- β -D-thiogalactoside (IPTG) for 3 h at 30°C. The recombinant proteins were eluted with 30 mM imidazole. TORC1 was prepared from yeast cells. In brief, *GFP-TOR1^{11954S}* cells were grown in YPD medium and treated with 50 μ g/mL cycloheximide for 15 min just before harvest. Cells were resuspended in lysis buffer (50 mM Tris-Cl (pH 8.0), 400 mM NaCl, 10% glycerol, 1 mM dithiothreitol (DTT), 0.2% Triton X-100, 1 mM PMSF, Complete EDTA-free protease inhibitor cocktail (Roche), PhosSTOP (Roche)) and were lysed with a glass bead homogenizer. The cleared cell extract was then incubated with GFP-Trap magnetic beads (Proteintech) for 2 h at 4°C. After intensive washing of the beads, the bound TORC1 was used in the *in vitro* phosphorylation experiment. The phosphorylation reactions were performed in 25 mM HEPES (pH 7.4), 100 mM NaCl, 10 mM MgCl₂, 1 mM MnCl₂, 1 mM DTT, 10 mM ATP. Reactions were incubated for 1 h at 30°C. The reactions were terminated in Laemmli buffer (250 mM Tris-Cl (pH 6.8), 8% SDS, 10% glycerol, 5% β -mercaptoethanol, traces of bromophenol blue) by heating for 5 min at 95°C, and proteins were resolved by SDS-PAGE containing 20 μ M Phos-tag (Fujifilm).

Cell lysate preparation and Western blot analysis

Cells lysates were prepared as previously reported with slight modifications.³ Briefly, two OD₆₀₀ units of cells were harvested and treated with 10% trichloroacetic acid for at least 15 min on ice. The precipitated protein was pelleted by centrifugation at 20,000 \times g for 15 min at 4°C. The pellets were re-dissolved in 50 μ L of high urea buffer (HU buffer: 8 M urea, 5% SDS, 1 mM EDTA, 200 mM sodium phosphate (pH 6.8), 100 mM DTT, traces of bromophenol blue). Cells were lysed using a FastPrep instrument (MP-Biomedicals) with 0.5-mm zirconia beads for three cycles (speed 5.0 for 20 s), followed by heating for 15 min at 65°C and vortexing for 2 min. The cell lysates were centrifuged at 20,000 \times g for 5 min and subjected to SDS-PAGE and Western blot analysis using the indicated antibodies.

Immunoprecipitation experiments

Cells were resuspended in TAP-A buffer (50 mM Tris-HCl (pH 8.0), 150 mM NaCl, 10% glycerol, 1 mM DTT, 1 mM PMSF, 1 μ M microcystin-LR, PhosSTOP, and 1 mM EDTA supplemented with Complete EDTA-free protease inhibitor cocktail) and lysed with a FastPrep instrument (MP-Biomedicals) and 0.5-mm zirconia beads. After lysis, cell lysates were incubated with Triton X-100 (0.2% final concentration) for 10 min at 4°C, and then clarified by centrifugation at 20,000 \times g for 10 min at 4°C. Gtr1-TAP or TAP-Tor1 proteins were precipitated with magnetic beads covalently coupled to rabbit IgG (Dynabeads M-270 Epoxy beads: Invitrogen) at 4°C. GFP-Pib2 proteins were precipitated with magnetic GFP-Trap-M beads (Chromotek) at 4°C. The beads were washed three times with TAP-A buffer containing 0.2% Triton X-100. If indicated, all immunoprecipitation buffers were added with the specified final concentration of L-cysteine, D-cysteine, L-leucine, or L-methionine. If indicated, L-cysteine was added to the immunoprecipitation buffers at a final concentration of 30 mM. Bound proteins were eluted from beads by heating for 15 min at 65°C in high-urea buffer, then subjected to SDS-PAGE and Western blot analysis.

Quantitative analyses of the blots were performed using ImageJ software when necessary.

Protein purification

E. coli Rosetta 2 (DE3) carrying pGEX-6P-1(+)-derived plasmids were grown in LB medium containing 50 μ g mL⁻¹ ampicillin and 25 μ g mL⁻¹ chloramphenicol at 37°C overnight. The bacterial culture was diluted to an OD₆₀₀ of 0.1 in LB medium containing

50 $\mu\text{g mL}^{-1}$ ampicillin and 25 $\mu\text{g mL}^{-1}$ chloramphenicol, and then cultured to an OD_{600} of 0.7 at 37°C. The bacterial culture was incubated on ice for 30 min before the addition of IPTG. Expression was induced by 0.25 mM IPTG at 23°C for 6 h. Cells were collected, suspended in lysis buffer (50 mM Tris-HCl (pH 8.0), 150 mM NaCl, 10% glycerol, 1 mM DTT, 1 mM PMSF, and 1 mM EDTA supplemented with Complete EDTA-free protease inhibitor cocktail), and lysed by sonication (Ampl: 40%; 0.7 s on/0.3 s off; 30 cycles). Then lysates were incubated with Triton X-100 (0.2% final concentration) for 10 min at 4°C and clarified by centrifugation at 20,000 $\times g$ for 10 min at 4°C. The GST-tagged proteins were incubated with glutathione Sepharose beads for 2 h at 4°C, washed with TAP-B buffer (50 mM Tris-HCl (pH 8.0), 150 mM NaCl, 10% glycerol, 1 mM EDTA, 1 mM DTT), and eluted with elution buffer (50 mM Tris-HCl (pH 8.0), 150 mM NaCl, 10% glycerol, 1 mM EDTA, 1 mM DTT, 20 mM reduced glutathione). Proteins immobilized on the beads were eluted with Laemmli buffer by heating for 5 min at 95°C. Protein samples were resolved by SDS-PAGE and CBB staining.

In vitro binding assay

To examine Pib2-Tor1 interaction in response to changes in cysteine levels, TAP-Tor1 was purified from TAP-Tor1-expressing yeast as described above. GST-tagged Pib2(304–635) was purified from *E. coli* Rosetta 2 (DE3) as described above. Purified TAP-Tor1 on magnetic beads was suspended in pull-down buffer (50 mM Tris-HCl (pH 8.0), 150 mM NaCl, 10% glycerol, 1 mM EDTA, 1 mM DTT), mixed with GST-Pib2(304–635) along with the indicated concentration of L-cysteine, D-cysteine, or L-methionine, and then rotated for 3 h at 4°C. Following this, the magnetic beads were washed three times with pull-down buffer, suspended in HU buffer, and heated for 15 min at 65°C. Proteins were separated using SDS-PAGE and analyzed by immunoblotting.

Cysteine uptake assay

Radiolabeled amino acid uptake was performed as previously reported with slight modifications.^{42,43,66} Briefly, cells were grown in SCD medium until mid-log phase, followed by nitrogen starvation using SD-N medium for 30 min. Cells were harvested and suspended in 300 μL SD-N medium. The assay medium contained 0.35 $\mu\text{Ci L}^{-1}$ [³⁵S]-cysteine in SD-N medium and a final concentration of 0.25 mM of cysteine, and was warmed to 30°C. The cysteine uptake assay was initiated by the addition of 100 μL of pre-warmed cell suspension to 100 μL of assay medium and then incubated for 5 min at 30°C. The uptake assay was stopped by adding 1 mL SD-N medium with 25 mM L-cysteine. The cells were collected on a glass-fiber filter (Cytiva, 1827-025) by aspiration and washed three times with SD-N medium with 0.25 mM L-cysteine. The filter was immersed in 3 mL of scintillation fluid and radioactivity was measured using a liquid scintillation counter (Tri-Carb 2810 TR, PerkinElmer). Background activity was determined by following the same procedure as in the experimental group described above, but without adding any cells. The amount of accumulated compound was calculated as previously reported.⁶⁶

Cysteine-binding assay and K_d calculation

Amino acid binding assays were performed as previously reported.²² GST-Pib2(304–635), GST-Pib2(440–635), GST-Pib2(304–620), GST-Pib2(304–635), GST-Pib2(304–635) mutant (W632A), and GST-Pib2(304–635) mutant (F635A) proteins were expressed in *E. coli* Rosetta 2 (DE3) by induction with 0.25 mM IPTG for 6 h at 23°C. Following purification of the GST-tagged protein, the glutathione Sepharose beads were washed four times with TAP-B buffer (50 mM Tris-HCl (pH 8.0), 150 mM NaCl, 10% glycerol, 1 mM EDTA, 1 mM DTT), and a portion of the purified protein was analyzed by SDS-PAGE and CBB staining. The beads were suspended in 200 μL TAP-B buffer and incubated for 3 h on ice with the indicated amounts of L-[³⁵S]-cysteine and unlabeled cysteine. After incubation, the beads were washed four times with TAP-B buffer and resuspended in 900 μL TAP-B buffer, and then 300- μL aliquots were separately added to 3 mL scintillation fluid. The radioactivity was measured using a liquid scintillation counter (Tri-Carb 2810 TR, PerkinElmer).

The affinity of Pib2 for cysteine was determined as previously reported.²²

LC-MS analysis

Cells expressing GFP-Pib2 were grown in SCD medium until mid-log phase, followed by nitrogen starvation using SD-N medium for 30 min, and then restimulated with or without 5 mM cysteine for 15 min. GFP-Pib2 was immunoprecipitated as previously described. GFP-Pib2 was eluted from beads by heating for 15 min at 65°C in HU buffer, then subjected to SDS-PAGE and CBB staining. The subsequent sample preparation and LC-MS assay were performed by the CoMIT Omics Center of the Graduate School of Medicine at Osaka University. The abundance of each protein was quantified using the exponentially modified Protein Abundance Index (emPAI), which estimates the absolute protein abundance based on the number of peptides identified by MS.⁶⁷

QUANTIFICATION AND STATISTICAL ANALYSIS

Data were analyzed using unpaired *t* test in GraphPad Prism (San Diego, CA, USA). Details were presented in each figure legend.